REPUBLIC OF TURKEY
YILDIZ TECHNICAL UNIVERSITY
GRADUATE SCHOOL OF NATURAL AND APPLIED SCIENCES

DYNAMIC PROGRAMMING-BASED MULTI-VEHICLE LONGITUDINAL TRAJECTORY OPTIMIZATION

CAFER AVCI

Ph.D. THESIS
DEPARTMENT OF COMPUTER ENGINEERING
PROGRAM OF COMPUTER ENGINEERING

ADVISER
PROF. DR. NİZAMETTİN AYDIN

İSTANBUL, 2018

REPUBLIC OF TURKEY

YILDIZ TECHNICAL UNIVERSITY

GRADUATE SCHOOL OF NATURAL AND APPLIED SCIENCES

DYNAMIC PROGRAMMING-BASED MULTI-VEHICLE LONGITUDINAL TRAJECTORY OPTIMIZATION

A thesis submitted by Cafer AVCI in partial fulfillment of the requirements for the degree of **PHILOSOPHY OF DOCTORATE** is approved by the committee on 16.05.2018 in Department of Computer Engineering, Computer Engineering Program.

Thesis Adviser

Prof. Dr. Nizamettin AYDIN

Yıldız Technical University

Approved By the Examining Committee

Prof. Dr. Nizamettin AYDIN

Yıldız Technical University

Prof. Dr. Selim AKYOKUŞ, Member

Dogus University

Assoc. Prof. Dr. Veli HAKKOYMAZ, Member

Yıldız Technical University

Assoc. Prof. Dr. Mehmet S. AKTAŞ, Member

Yıldız Technical University

Assoc. Prof. Dr. Müjdat SOYTÜRK, Member

Marmara University

This study was supported by the Scientific and Technological Research Council of Turkey (TUBITAK) Grant No: 1059B141500634.

ACKNOWLEDGEMENTS

Firstly, I would like to express my deep and sincere gratitude to my advisor Dr.Nizamettin Aydın, Professor, Departmet of Computer Engineering, Yıldız Technical University, for his valuable support, consultation and motivation to finish my Ph.D. study.

I am very grateful to Dr.Xuesong Zhou, Assoc.Professor, Department of Civil and Enviromental Engineering, Arizona State University, for his great guidance in modelling and optimizing of cooperative autonomous vehicles and support throughout research. It is a great privilege and honor to work and study under his guidance.

I am extremely grateful to Baloka Belezamo, Ms.C, P.Eng., Ph.D(c), Arizona Department of Transportation, State of Arizona, for his vision on transportation science, friendship, empathy, and great sense of humor.

I would also like to thank all my friends for making my graduate studies experience pleasant and enjoyable, especially Thad K. Metz, Dr.Jiangtao Liu, Dr. Abit Balın, Dr. Hasan Badem and Dr. Pengfei Li.

Words cannot express the feelings I have for my parents for their constant unconditional support, I would not have made it this far without them. I am also greatly indebted to my wife for her patience and support.

Finally, I would like to express my acknowledgements to everyone who helped me during my Ph.D. study and in my life.

May, 2018

Cafer AVCI

TABLE OF CONTENTS

Page

LIST OF SYMBOLS vii

LIST OF ABBREVIATIONS viii

LIST OF FIGURES ix

LIST OF TABLES xi

ABSTRACT xii

ÖZET xiv

CHAPTER 1

INTRODUCTION 1

1.1 Autonomous Vehicle Levels Definition 3
1.2 Literature Review 5
1.2.1 Review of car-following models and AVs' impact on traffic flow characteristics 5
1.2.2 Review of vehicle trajectory optimization models 7
1.3 Objective of the Thesis 10
1.4 Hypothesis 10
1.5 Organization of the Thesis 11

CHAPTER 2

MODELLING SIMPLIFIED CAR-FOLLOWING BEHAVIOUR 13

2.1 Simplified car-following behavior for AV 13
2.2 Model leader-follower behavior in multi-AV formation control with changeable reaction times 18
2.3 Probability density function (PDF) of communication delay and its impact on driving risk 23

CHAPTER 3

DYNAMIC PROGRAMMING FOR MULTIPLE VEHICLE TRAJECTORY OPTIMIZATION WITH CHANGEABLE REACTION TIMES IN A PLATOON 29

3.1 An overview of Dynamic Programming 29
3.1.1 Mathematical Formulation 30
3.1.2 Optimal Control Action 31
3.2 Different models and control variables 32
3.3 Formulation and Optimality Conditions in Dynamic Programming for Coupled Vehicles 35
3.4 Dynamic programming algorithms 39
3.4.1 Mode (“1”) 39
3.4.2 Mode (“1+1”) 40
3.4.3 Mode (“1+m”) 41
3.4.4 Mode (“1+m(w)”) 42
3.5 Time complexity of algorithms 44
3.6 Improving computational complexity 45

CHAPTER 4

NUMERICAL EXPERIMENTS 48

4.1 Trajectory Analysis of one AV by Using Mode “1” 49
4.2 Trajectory Analysis of two simultaneous AVs by Using Mode “1+1” 50
4.3 Platoon Analysis by Using Mode “1 + M” for Automated Vehicles with Surrounding Obstacles 51
4.4 Platoon Analysis by using Mode “1 + m (w)” 54

CHAPTER 5

RESULTS AND DISCUSSION 58

5.1 Answers to the research questions 58
5.2 Future works and discussions 59

REFERENCES 60

APPENDIX-A 67

POSSIBLE EXTENSION TO MULTI-PLATOON MERGING CONTROL 67

CURRICULUM VITAE 69

LIST OF SYMBOLS

L	Length of vehicle (e.g., 20 feet or 4 meters)
d_n	Minimum distance between the front of the leading car and the following car
d_0	The minimum safe rear-to-end distance after an emergency braking event
v_f	Maximum or free-flow driving speed
$x_n(t)$	The position of following vehicles
$x_{n-1}(t)$	The position of lead vehicles
S_n	Distance headway between the positions of leading and following vehicles
v_n	Speed of the vehicle n
a_n	The deceleration rate of vehicle n
$I_n(t)$	Time headway between n^{th} and $(n-1)^{th}$ vehicles
τ_{PR}	Perception-response time (PRT)
τ_n	Slope in a linear spacing-speed function
τ_B	Redundant time buffer used in linear car following model for AV
k_{jam}	Jam density
w_b	Backward wave speed

LIST OF ABBREVIATIONS

AHS	Automated Highway Systems
ACC	Adaptive Cruise Controller
ATM	Active Traffic Management
AV	Automated Vehicle
CACC	Cooperative Adaptive Cruise Control
CAV	Connected and Automated Vehicles
CPU	Central Processing Unit
DP	Dynamic Programming
DSRC	Dedicated Short Range Communication
GPU	Graphic Processing Unit
IDM	Intelligent Driver Model
MILP	Mixed Integer Linear Programming
MSR	Maximum Service Rate
NGSIM	Next Generation Simulation
PDF	Probability Density Function
UAV	Unmanned Aerial Vehicles
USDOT	United States Department of Transportation
V2V	Vehicle-to-Vehicle

LIST OF FIGURES

Page

Figure 1.1 A representation of connected vehicles and infrastructure ([3]) 2
Figure 1.2 Society of Automotive Engineer International's six levels of automation.. 3
Figure 2.1 The process of car-following behavior change..... 15
Figure 2.2 Relation between spacing and velocity and piecewise linear approximation to vehicle trajectories with a speed change (adapted from Newell [17]) .. 16
Figure 2.3 Vehicles' trajectory based on simplified car following model..... 18
Figure 2.4 Vehicles' trajectory from free flow speed to congested speed..... 19
Figure 2.5 Vehicles' trajectory from congested speed to free-flow speed..... 20
Figure 2.6 Constant reaction time, speed is changing from 60 mph to 30 mph and from 30 mph to 60 mph..... 20
Figure 2.7 Reaction time changing constraints..... 21
Figure 2.8 Speed limit for transition process 21
Figure 2.9 Reaction time is changing with $\tau 1$ = 1.5 s, $\tau 2$ = 1 s, $\tau 3$ = 0.5 s, $\tau 4$ = 0 s without defining speed limit 22
Figure 2.10 Reaction time is changing with $\tau 1$ = 1.5 s, $\tau 2$ = 1 s, $\tau 3$ = 0.5 s, $\tau 4$ = 0 s with defining speed limit 22
Figure 2.11 PDF of reaction times..... 24
Figure 2.12 Relation between spatial distance and time considering response time lag (adapted from [66])..... 25
Figure 2.13 Layout of hypothetical road segment of space and time axes for 3D illustration of trajectories..... 26
Figure 2.14 3D illustration of trajectories of AVs' and reaction time changing at the critical bottlenecks..... 27
Figure 3.1 Principle of optimality; as M is on the optimal path from O to D, the optimal path from M to D is what remains of the same path. *t* is time and *x* is the state of the system 29
Figure 3.2 Optimal paths for all initial states *x* from time *n+1* to *D* are known. Which is of the actions uj is optimal path from O to D 30
Figure 3.3 Discretized space-time network for vehicle trajectory optimization for (1) 33
Figure 3.4 Discretized space-time network for vehicle trajectory optimization for (1+1) 33
Figure 3.5 Discretized space-time network for vehicle trajectory optimization for (1+m) 34
Figure 3.6 Discretized space-time network for vehicle trajectory optimization (1+m(w))..... 34

Figure 3.7 Illustration of maximum completion time 38
Figure 3.8 Illustration of full search space for mode 1+m(w) 45
Figure 3.9 Illustration of reduced search space for mode 1+m(w) 45
Figure 3.10 Illustration of reduced search space with optimized step size for mode 1+m(w) 46
Figure 4.1 Hypothetical environment for the experiments for Modes “1” and “1+1” 48
Figure 4.2 Optimal trajectory for Mode “1” 49
Figure 4.3 Optimal trajectories for Mode “1+1” 50
Figure 4.4 Hypothetical layout of experiments 51
Figure 4.5 Human-operated vehicle trajectories for NGSIM data 101 lane 1 52
Figure 4.6 Human-operated vehicle trajectories for NGSIM data 101 lane 2 52
Figure 4.7 Mixed traffic conditions when reaction time equals 0.5 s for lane 1 53
Figure 4.8 Mixed traffic conditions when reaction time equals 0.5 s for lane 2 53
Figure 4.9 Zooming view of mixed traffic conditions which highlighted in Figure 4.7 for lane 1 54
Figure 4.10 Zooming view of mixed traffic conditions which highlighted in Figure 4.8 for lane 2 54
Figure 4.11: Layout of hypothetical road segment 55
Figure 4.13: Optimal vehicle trajectories by using mode ‘1+m(w)’ with enforcing speed limit for leading vehicle in transition process 56
Figure A.1. Illustration of merging process by using multi-platoon formation control 68

LIST OF TABLES

Page

Table 2.1 Different interpretations of linear car following model $\boldsymbol{S_n = \tau_n \times v_n + d_n}$ with sample settings 17
Table 2.2 Service rates at the critical bottlenecks..... 28
Table 3.1 Description of different modes..... 32
Table 3.2 All elements of dynamic programming for all optimization types..... 35
Table 3.3 Processing time for three different cases..... 47
Table 4.1 MSR (vphpl) by using different reaction times with moving obstacles. ... 53

ABSTRACT

DYNAMIC PROGRAMMING-BASED MULTI-VEHICLE LONGITUDINAL TRAJECTORY OPTIMIZATION

Cafer AVCI

Department of Computer Engineering

Ph.D. Thesis

Adviser: Prof. Dr. Nizamettin AYDIN

The current key trend of technological revolution seeks to impact the system through vehicle-based revolution. As population, economic growth and personal travel activities continue to increase, traffic congestion remains as an extremely challenging problem due to limited road capacity and limited budgets for expanding infrastructure. Therefore there is significant interest in intelligent vehicles profits connectivity that offer opportunities for reduced emissions and clean energy sources. A recently emerging technology, autonomous vehicles or automated vehicles (AV) are likely to create a revolutionary paradigm shift in the near future for real-time traffic system automation and control. AV technology is expected to provide a wide range of new opportunities for managing transportation networks, and also redefines what is tractable regarding full system-wide optimization through a tight integration among vehicles and system managers. One of the most obvious benefits of AV is to improve the productivity of drivers by enabling the drivers to do something else than driving. However, it is clear that the driving environment and driver-vehicle interactions are expected to change, with the introduction of connected automated vehicles (CAV). Jointly optimizing multi-vehicle trajectories is a critical task in the next-generation transportation system with autonomous and connected vehicles. Based on a space-time lattice, it is presented a set of integer programming and dynamic programming models for scheduling longitudinal trajectories, where the goal is to consider both system-wide safety and throughput requirements under supports of various communication technologies. Newell's simplified linear car following model is used to characterize interactions and collision avoidance between vehicles, and a control variable of time-dependent platoon-level reaction time is introduced in this study to reflect various degrees of vehicle-to-vehicle or vehicle-to-infrastructure communication connectivity. By adjusting the lead vehicle's speed and platoon-level reaction time at each time step, the proposed optimization models could

effectively control the complete set of trajectories in a platoon, along traffic backward propagation waves. This parsimonious multi-vehicle state representation sheds new lights on forming tight and adaptive vehicle platoons at a capacity bottleneck. It is examined the principle of optimality conditions and resulting computational complexity under different coupling conditions.

Key words: Traffic flow management, autonomous vehicle, vehicle trajectory optimization, car-following model, dynamic programming

ÖZET

DİNAMİK PROGRAMLAMA TABANLI ÇOKLU ARAÇLAR İÇİN BOYLAMSAL YÖRÜNGE OPTİMİZASYONU

Cafer AVCI

Bilgisayar Mühendisliği Anabilim Dalı

Doktora Tezi

Tez Danışmanı: Prof. Dr. Nizamettin AYDIN

Teknolojik devrimin şu anki anahtar eğilimi, araç tabanlı sistemi araç tabanlı devrim yoluyla etkilemeye çalışıyor. Nüfus, ekonomik büyüme ve kişisel seyahat faaliyetleri arttıkça, sınırlı trafik kapasitesi ve altyapıyı genişletmek için sınırlı bütçeler nedeniyle trafik sıkışıklığı son derece zorlu bir sorun olarak kalmaya devam etmektedir. Bu nedenle, azaltılmış emisyonlar ve temiz enerji kaynakları için fırsatlar sunan akıllı araçların yararlığına ilişkin önemli bir ilgi vardır. Yakın zamanda ortaya çıkan teknoloji, otonom araçlar veya otomatik araçlar, gerçek zamanlı trafik sistemi otomasyonu ve kontrolü için yakın gelecekte devrimci bir paradigma kayması yaratacaktır. Otonom araç teknolojisinin, ulaştırma ağlarını yönetmek için geniş bir yelpazede yeni fırsatlar sunması ve ayrıca, sistem ve sistem yöneticileri arasında sıkı bir entegrasyonla sistem genelinde optimizasyonla ilgili olarak neyin takip edilebileceğini yeniden tanımlaması bekleniyor. Otonom aracın en belirgin faydalarından biri, sürücülerin sürüşten başka bir şey yapmasını sağlayarak sürücülerin verimliliğini arttırmaktır. Bununla birlikte, sürüş ortamının ve sürücü-araç etkileşimlerinin, kooperatif otonom araçların devreye girmesiyle değişmesi beklenmektedir. Çok araçlı yörüngeleri ortaklaşa optimize etmek, otonom ve kooperatif araçlarla birlikte gelecek nesil ulaşım sisteminde kritik bir görevdir. Bir uzay-zaman örgüsüne dayanarak, çeşitli iletişim teknolojilerinin destekleri altında hem sistem çapında güvenlik ve işlem gereksinimlerini göz önüne almak hem de uzunlamasına yörüngeleri planlamak için bir dinamik programlama modeli sunulmuştur. Newell'in basitleştirilmiş lineer otomobil modeli, araçlar arasındaki etkileşimleri ve çarpışmayı önleme özelliklerini tanımlamak için kullanılmıştır ve bu çalışmada araçtan araçlara veya araçtan aracıya aktarılan araçların çeşitli seviyelerini yansıtacak şekilde, zamana bağlı olarak reaksiyon süresi kontrol değişkenleri sunulmuştur. Lider araç hızını ve takım reaksiyon zamanını her bir zaman adımında ayarlayarak, önerilen optimizasyon modelleri trafik geri yayılım dalgaları boyunca bir takımdaki tüm yörünge dizilerini etkili

bir şekilde kontrol etmektedir. Bu çok yönlü çok araçlı durum gösterimi kapasite darboğazında sıkı ve uyarlanabilir araç takımları oluşturma konusunda yeni bir bakış açısı sunmaktadır. Farklı bağlanma koşulları altında uygunluk koşullarının ve sonuçtaki hesaplama karmaşıklığı incelenmiştir.

Anahtar Kelimeler: Trafik akım yönetimi, otonom araç, araç yörünge optimizasyonu, araç-takip modeli, dinamik programlama

CHAPTER 1

INTRODUCTION

Rapid developments in technologies and transportation science have been integrative impact on to the evolution of daily life [1]. This impact have seen considerable integration of advances in communication, digital processing and sensing technologies in transportation science providing enhancement in efficiency, safety, sustainability and reliability. The next key trend of technological revolution seeks to impact the system through vehicle-based revolution. As population, economic growth and personal travel activities continue to increase, traffic congestion remains as an extremely challenging problem due to limited road capacity and limited budgets for expanding infrastructure. Therefore there is significant interest in intelligent vehicles profits connectivity that offer opportunities for reduced emissions and clean energy sources. A recently emerging technology, autonomous vehicles or automated vehicles (AV) are likely to create a revolutionary paradigm shift in the near future for real-time traffic system automation and control. AV technology is expected to provide a wide range of new opportunities for managing transportation networks, and also redefines what is tractable regarding full system-wide optimization through a tight integration among vehicles and system managers. It is estimated that the direct societal value that will be produced will be between 0.2 and 1.9 trillion dollars annually by 2025 [2]. Such positive impacts are the driving forces behind the emergence of AV technology, making it a viable, economic model in the near future and beyond. AV have been modelled with significant advances in sensing, pattern recognition and control technologies including widespread wireless communication technologies providing an internet of vehicles that can communicate with other intelligent vehicles (using Vehicle-to-Vehicle (V2V) communications) and the infrastructure (using Vehicle-to-Infrastructure (V2I) communications).

One of the most obvious benefits of AV is to improve the productivity of drivers by enabling the drivers to do something else than driving. However, it is clear that the driving environment and driver-vehicle interactions are expected to change, with the introduction of connected automated vehicles (CAV). Human-driven vehicles and AV have different driving parameters in scale related to varying capabilities, for example human driving vehicle has a higher reaction time compared to AV. The idea of autonomous vehicles, better known as "self-driving cars," are becoming increasingly popular in the modern world. Each year, cars are able to do more by themselves. In theory, fully self-driving cars would be purely beneficial to society. In current transportation practices, drivers are at the mercy of their own abilities, as well as those of others on the road. Drunk driving, lack of driver awareness, and slow reaction times contribute to many accidents and fatalities. If cars drove themselves, it would eliminate the human aspect that is prone to error.

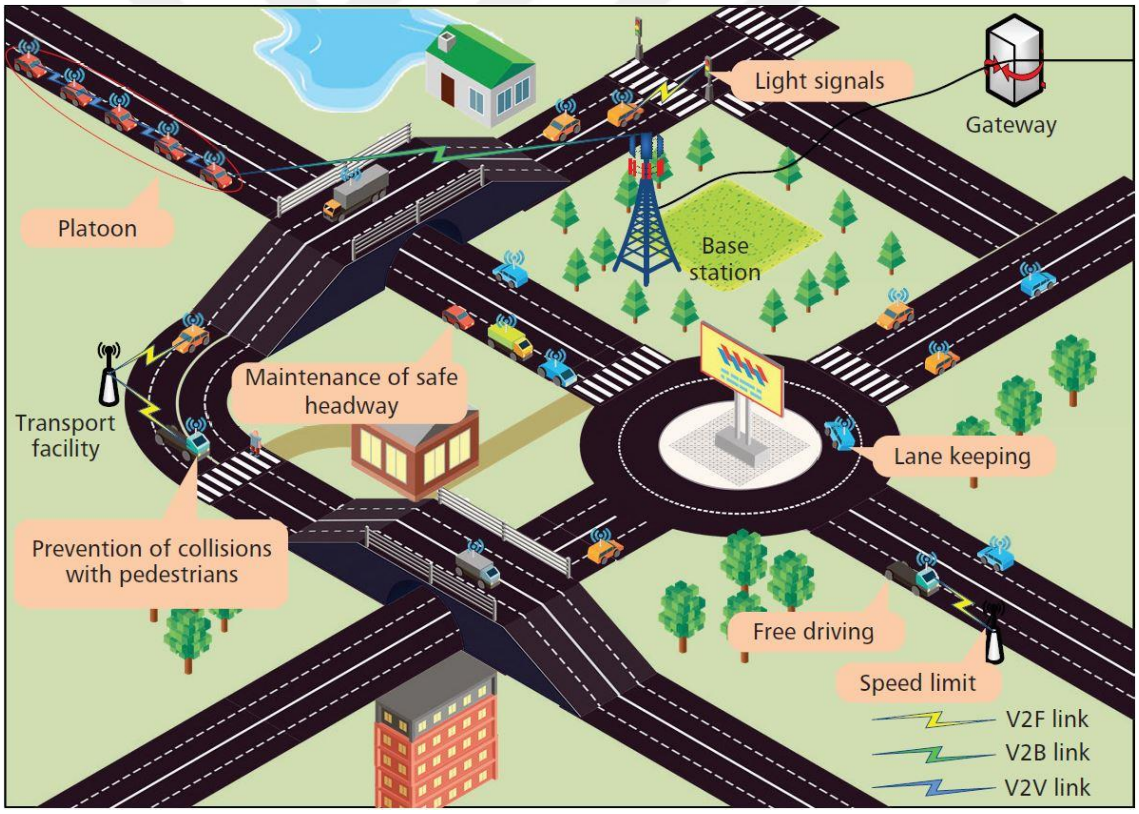


Figure 1.1 A representation of connected vehicles and infrastructure ([3])

Figure 1.1 shows a conceptual representation of a connected environment for AV. Some of beneficial AV applications are shown as conceptual representation in Figure 1.1 such as prevention of collisions with pedestrians, lane keeping, satisfying speed limit, integrated light signal at intersections, cooperative autonomous driving, etc. Each of these

applications is or has been the subject of extensive research in various fields. As such, AV technology could be considered at the junctions of many disciplines such as transportation science, information technology, electrical engineering, software and hardware engineering, law, ethics, and philosophy. In this research, cooperative autonomous driving is examined from a transportation and information technology points of view.

1.1 Autonomous Vehicle Levels Definition

Before going forward, it is important to outline terminology being used in literature and also in this research. The broad term "autonomous" can encompass varying amounts of automated control. For this reason, in September 2016, the levels were defined by The United States Department of Transportation (USDOT) announced that it now uses Society of Automotive Engineer's (SAE) six level of automation in its Federal Automated Vehicles Policy report [4], [5]. Visual representations of SAE's six levels of automation definitions are shown in Figure 1.2. The following automation levels summarize the SAE definitions:

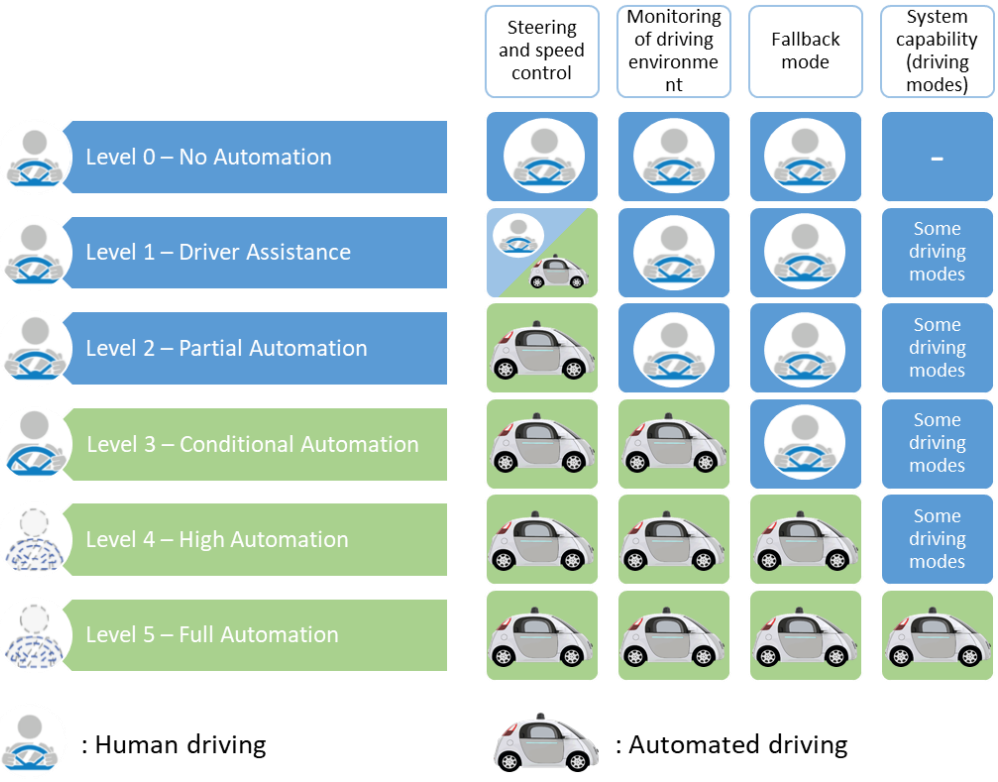


Figure 1.2 Society of Automotive Engineer International's six levels of automation

Level 0: No Automation. The full-time performance by the human driver of all aspects of the dynamic driving task, even when enhanced by warning or intervention systems

Level 1: Driver Assistance. The driving mode-specific execution by a driver assistance system of either steering or acceleration/deceleration using information about the driving environment and with the expectation that the human driver performs all remaining aspects of the dynamic driving task.

Level 2: Partial Automation. The driving mode-specific execution by one or more driver assistance systems of both steering and acceleration/deceleration using information about the driving environment and with the expectation that the human driver performs all remaining aspects of the dynamic driving task.

Level 3: Conditional Automation. The driving mode-specific performance by an Automated Driving System of all aspects of the dynamic driving task with the expectation that the human driver will respond appropriately to a request to intervene.

Level 4: High Automation. The driving mode-specific performance by an Automated Driving System of all aspects of the dynamic driving task, even if a human driver does not respond appropriately to a request to intervene.

Level 5: Full Automation. The full-time performance by an Automated Driving System of all aspects of the dynamic driving task under all roadway and environmental conditions that can be managed by a human driver.

These levels of automation provide consistent terminology for use by transportation professionals, policymakers and researchers. While the National Highway Traffic Safety Administration (NHTSA) has developed an alternative 5-level (0-4) framework of driving automation for on-road vehicles [4], all discussions used in this document will refer to SAE′s definitions.

Autonomous vehicle capabilities are often discussed in conjunction with connected vehicle systems. The two are in effect distinct. The former is envisioned as the ability to drive with no external assistance, possible through extensive sensing and massive intelligence fully residing within the vehicle. All these functions could be enhanced through connectivity, e.g., when neighboring vehicles and/or the infrastructure convey messages to other vehicles about respective locations, road features, or control displays. Additional coordinated strategies could thus be enabled to further enhance safety and flow quality. However, in that case more of the intelligence resides in the infrastructure, or the vehicle-infrastructure system instead of residing exclusively within individual vehicles.

These factors have important implications for deployment, coordination, vulnerability, and resilience of the associated system. Most notably, connected vehicle systems require a much greater degree of coordination among auto manufacturers and traffic management authorities (generally public sector), whereas autonomous vehicles are envisioned as fully self-sufficient.

1.2 Literature Review

Varaiya outlined an automated highway systems (AHS) to significantly improve highway capacity and safety, in which a hierarchical control mechanism for AVs is provided at different spatial scales, ranging from a network, routes, freeway corridors, to dedicated lanes [6]. In a recent review from the perspective of traffic flow theory and operations, Mahmassani highlighted many unique features and challenges in the next-generation transportation systems of optimizing and controlling automated and connected vehicles [7]. In the connected environment with different degrees of automation and connectivity supports, we need to not only fully recognize the changing driver/vehicle behavior (including car following and lane-changing), but also design a system-optimal scheduling and control architecture to achieve robust, stable and effective traffic flow management.

In this research, it is focused on a longitude vehicle trajectory optimization problem, which is fundamental to many AV applications, such as vehicle platooning or adaptive cruise control. The related research topics are briefly reviewed, including car following models and traffic-flow oriented trajectory optimization.

1.2.1 Review of car-following models and AVs' impact on traffic flow characteristics

Since the 1950s, there are a wide range of car following models proposed for vehicles driven by humans. After the earliest car-following models developed by Reuschel and Pipes, many car-following models were developed based on the response-stimulus mechanism between a lead vehicle and a following vehicle [8], [9]. As examples, Kometani and Sasaki [10], [11], [12]. Forbes et al., Forbes, and Chandler et al. had developed nonlinear car-following models, respectively [13], [14], [15]. To overcome the complexity of those nonlinear models, Newell first presented a simplified car-following theory which is consistent with the macroscopic triangular flow-density relationship [16], [17]. Due to its simplicity without loss of flexibility, the Newell's simplified car-following models have been calibrated in many locations using real-world trajectory data.

For example, Ahn el al. calibrated the Newell's car-following model using real-world vehicle trajectory data at signalized intersections [18]. Taylor et al. applied the time-warping approach to investigate drivers' situation-dependent perception and reaction to external impetus [19]. In parallel, there are also many studies focusing on calibrating various stochastic and situation-dependent car-following models, to name a few, Hamdar et al. [20], Laval and Leclercq [21], Hoogendoorn et al. and Kim and Mahmassani [22], [23].

While most car-following models focus on human-operated vehicles, researchers in automated control and artificial intelligence started characterizing the driving behaviors of AVs and their potential impact on road capacity in the 1990s. Reliable actuators and sensors in AVs, as summarized by Ward, have made AVs more available and ready for field tests [24]. There are two types of research efforts in parallel along this research line: one focusing on the interactions between AVs based on vehicle dynamics to derive possible changes to traffic characteristics; the other focusing on overall changes to the performance of road capacities brought by AVs under various conditions. As examples of the first type of research, Horowitz and Varaiya described the findings from the automated highway system (AHS) development in the 1990s at the California PATH program [25]. In general, the actuators make AVs react much faster than a normal or even sensitive human driver. Sensitive drivers can have a short perception-reaction time of 1.0 s to 1.5 s, as reported by NAHSC, compared to a typical perception-reaction time of 2.0-2.5 s [26]. Further shorter AV reaction times, such as 0.7 s reported by Bose and Ioannou, can lead to closer spacing between cars and a higher roadway capacity [27]. Another important aspect that motivates the development of AHS is based on optimal flow control through reducing or smoothing random errors in human drivers via the deterministic and possibly optimized vehicle trajectory planning/control. An early prototype for single-lane vehicle platooning on automated highways was reported by Alvarez and Horowitz [28]. They designed a safe zone between two platoons according to the distance, relative speed and maximum acceleration and deceleration rates. Horowitz and Varaiya also evaluated many platooning methods in simulation as well as in the physical test beds [25]. Recently, Lioris et al. demonstrate that platoons of connected vehicles can double throughput in urban roads based on by the analysis of three queuing models and by the simulation of a road network with 16 intersections and 73 links [29].

A set of adaptive cruise controller (ACC) and the intelligent driver model controller (IDM by Treiber et al.) were tested by Milanés and Shladover in different traffic situations in order to measure the actual responses of the vehicles [30, 31]. Talebpour and Mahmassani proposed a non-linear acceleration framework for autonomous vehicles and evaluated the possible changes to traffic flow stability [32]. Roncoli et al. proposed a linear lane-based traffic flow model and discussed how to calibrate the model and optimize the traffic flow in the presence of autonomous vehicles [33], [34]. Using the relaxed Pontryagin's minimum principle, Hu et al. proposed an optimal controller to improve fuel efficiency for a vehicle equipped with automatic transmission traveling on rolling terrain [35]. Recently, by applying the Improved Intelligent Driver Model (IIDM) in a road traffic simulation package named SUMO, Askari et al. assess the impact of the maximum vehicle acceleration and variable proportions of adaptive cruise control (ACC) and cooperative adaptive cruise control (CACC) vehicles on the throughput of an intersection [36]. The results show that (C)ACC vehicles can obviously increase the urban mobility with little or no cost in infrastructure.

1.2.2 Review of vehicle trajectory optimization models

Vehicle trajectory optimization and control has been extensively studied in a broader domain, including surface vehicles, aircraft and Unmanned Aerial Vehicles (UAV). As summarized by Betts, nonlinear programming, optimal control, and dynamic programming are classical modeling approaches to describe vehicle dynamics with various constraints and boundary conditions [37]. Typical solution algorithms for single-vehicle trajectory optimization problems include direct shooting, indirect shooting, multiple shooting and direct/indirect transcription, where the last two methods aim to solve multipoint boundary value problems. By using a constrained optimization method on fuel consumption, He et al. proposed an approximation approach for providing advisory speed limit to drivers in the bottleneck [38]. Along this line, Wu et al. applied reduce electricity consumption of electric vehicles method in the intersection [39]. Focusing on the multi-vehicle trajectory coordination problem, Schouwenaars et al. proposed a mixed integer linear programming (MILP) model to use readily available linear programming or integer programming solvers such as CPLEX [40]. In their proposed model, a set of vehicles move from initial boundary states to final states, subject to obstacle and inter-vehicle collision avoidance constraints. Recent development along

this line can be found in the studies by Grotli and Johansen [41], Richards et al. [42] and Grotli and Johansen [43] for UAV trajectory coordination problems, which cover a richer set of vehicle dynamics, obstacle avoidance, task timing requirement and communication-connectivity constraints. In mobile leader–follower networks [36], [37], [38] Sun and Cassandras highlights the important features of continuously preserving connectivity in a convex mission space [44].

Dynamic programming (DP)-based algorithms have been one key theoretic foundation for single-vehicle trajectory optimization, and its formulation typically involves several modeling elements: (i) the boundary of the search scope or map, (ii) discretized space-time lattices, (iii) a path searching algorithm that can find a safe trajectory to reach the destination and meet certain global goals, such as minimal fuel consumption or minimal travel times. While the DP-based trajectory optimization can reach the exact optimum, it is often too slow for real-time applications involving multiple vehicles. To address this issue, Flint et al. proposed an approximate DP algorithm for multiple vehicles to cooperatively search for targets [45]. The dissertation by McNaughton [46], based on an AV system architecture described by Urmson et al. for the 2007 DARPA Urban Challenge (DUC) [47], proposed a novel five-dimensional search algorithm that recognizes kinematic and dynamic constraints in clearly defined spatial and temporal dimensions, and used graphics processing unit (GPU) to enable parallel search algorithms. Recent survey papers by Katrakazas et al. and Paden et al. reviewed the existing motion planning approaches for self-driving vehicles [48, 49].

In a very recent study by Zhou et al., they proposed a shooting heuristic algorithm to smooth trajectories of multiple automated and connected vehicles, where a time geography-oriented approach is innovatively combined with Newell's simplified car following model to consider safe vehicle driving boundaries [50]. Ma et al. further discussed the computational complexity and performance of their shooting algorithm in their preceding study [51]. Bang and Ahn [52] proposed an innovative framework to embed Newell's simplified car-following model with different reaction times for CAV in a spring-mass-damper system [53, 54]. Their proposed swarm intelligence model is able to systematically characterize CAV platoon formation and evolution, under light traffic conditions. Gong et al. (2016) recently developed a rigorous convex program with quadratic constraints for representing the nonlinear safety distance constraint among coupled vehicles [55]. To address the computational challenges, they used dual based

distributed algorithms to iteratively refine the trajectory solutions and capture the desired transient and asymptotic dynamics. Compared these recent studies, our paper focuses on how to develop (linear) integer programming and dynamic programming model in a discretized multi-vehicle space-time representation. The parsimonious coupled multi-vehicle state representation to be constructed aims to not only shed new lights on defining the transient dynamic progress for adaptive vehicle platoons, but also provide a traffic-flow-oriented modeling methodology for extending a wide range of dynamic programming based real-time vehicle trajectory control algorithms under heaving and light traffic conditions.

In many multi-robot path planning applications, a group of autonomous vehicles follow predefined trajectories moving in a formation, which offers many advantages such as reducing team-level cost, increasing the robustness, efficiency and flexibility of the system. Designing such a system in a dynamic environment with avoiding obstacles to make motion planning requires robust configuration and discrete transformations [56]. Survey papers by Murray and Chen & Wang review the cooperative control and formation control of multi-vehicles/robots [57], [58]. With global and individually defined goals with different performance functions, the problem (e.g., addressed in an early study [59]) typically aims to optimize multi-robot trajectories by controlling leader-follower trajectories, specifying a reference point and defining a virtual structure. Egerstedt and Hu presented a strategy on solving path following problem based on multi-agent formation specifying virtual leader tracks as the reference trajectory, and avoiding obstacles by following a reference path [60]. Focusing on minimizing system cost with a user-defined global function for using in D* incremental search algorithm [61], Guo and Parker proposed an optimal motion planning model based on searching path and velocity patterns with safety margins by using a multidimensional state approach, which covers system states such as start and goal positions, environmental aspects and communication with other robots [62].

In addition to optimizing the system performance, more inherently, the analysis on stability of the system and how to stabilize the system are also critical for controlling autonomous vehicles in traffic systems. Based on the given vehicle reference posture and velocities, Kanayama et al. proposed a stable tracking control rule for non-holonomic autonomous mobile robots to find the most reasonable velocities, and Lyapunov function was adopted to prove the stability of the proposed rule [63]. De Wit and Sordalen

analyzed the exponential stabilization of two-degree-of-freedom mobile robots with non-holonomic constraints by a specific class of piecewise continuous controllers [64]. Recently, Miao and Wang provided a time-dependent adaptive control scheme at the torque level to address the stabilization issue and tracking problem for unicycle mobile robots with unknown dynamic parameters depending on the instantaneous and past information of the reference velocities [65].

1.3 Objective of the Thesis

While previous studies in the areas of vehicle motion planning have made important contributions in various aspects, it is still critically important to develop mathematically rigorous optimization models and computationally tractable algorithms to (1) consider the dynamic effect of vehicle interactions and also (2) reach the full potential of many system-level performance measures such as throughput, capacity, stability and safety. Along this line, this research aims to address the following theoretical research questions.

1) How to adapt the current car-following models to model traffic interactions of automated vehicles based on available connectivity and automated functions, and in particular the dynamic process of tight platoon formation and system-level control?

2) How to develop a theoretically rigorous optimization model (e.g., in the form of dynamic programming models) which could be programmable using different programming languages? Desirable multi-vehicle trajectory optimization models should be able to not only satisfy critical operational constraints such as obstacle avoidance, but also recognize the inherent nature of car following behavior to optimize platoon-level or system-level performance.

3) How to design on-line trajectory optimization algorithms to improve the performance of coupled AVs in a platoon, under complex traffic conditions with time-dependent capacity bottlenecks and obstacles of moving trajectories?

1.4 Hypothesis

Since vehicle dynamics is nonlinear in nature, most existing AV controller designs involve sophisticated nonlinear feedback loops through time-continuous car following models. To provide tractable mathematical models for both offline and on-line vehicle trajectory optimization, we reformulate Newell's simplified car-following model in a discretized high-resolution space-time lattice. As a result, we could approximate the time-continuous vehicle trajectory control problem though a dynamic programming,

which enables a rich body of standard optimization algorithms such as branch and bound and column generations. To further develop a solid theoretical foundation for multi-vehicle optimal control and efficient on-line optimization processes, we develop a family of efficient DP algorithms to schedule the optimal trajectory for multiple vehicles in a platoon.

In particular, a new control variable of time-dependent platoon-level reaction time is introduced in this study to reflect various degrees of vehicle-to-vehicle or vehicle-to-infrastructure communication connectivity. By adjusting the leading vehicle's speed and (location-dependent) platoon-level reaction time at each time step, the proposed DP algorithms could effectively control the complete set of trajectories in a platoon, along traffic backward propagation waves. This parsimonious multi-vehicle state representation sheds new light on forming tight and adaptive vehicle platoons at a capacity bottleneck. As a reduced reaction time in a platoon is associated with potentially negative safety impact due to possible communication delay and failure, we also extend a model by Przybyla et al. to analytically evaluate the situational risk associated with communication delay [66]. By dynamically configuring vehicle reaction times that could form different slopes of backward waves, we hope a platoon with adaptive reaction times could better balance the goals of capacity throughput maximization and risk minimization, under complex driving and communication support conditions.

In this research, previous work of Wei et. al. [67] has been extended through the improving algorithms for tightly coupled of AVs in mixed traffic conditions and developing new optimization model which has changeable reaction time as new control variable for multiple AVs.

1.5 Organization of the Thesis

The rest of this thesis is organized as follows: In Chapter 2, it is described how to adapt the traffic flow theories developed by Newell [17] and related kinematic wave model to characterize the AVs' dynamic trajectories. Also it is described how to estimate the associated risk due to reduced reaction time threshold by defining probability density function. In Chapter 3, principles and mathematical foundations of dynamic programming are overviewed and a sequence of dynamic programming based solution algorithms are further developed for different scenarios to optimize the vehicle speed profiles as well as to predict the optimized vehicle's impact on the following AVs. In Chapter 4, it is

demonstrated the potential of optimal trajectory control for both a single AV and multiple AVs through numerical analysis. Finally, it is given final conclusions and discussions, and also planned possible future researches.

CHAPTER 2

MODELLING SIMPLIFIED CAR-FOLLOWING BEHAVIOUR

2.1 Simplified car-following behavior for AV

The notation used in this section is listed below.

L: length of vehicle (e.g., 20 feet or 4 meters)

d_n: minimum distance between the front of the leading car and the front of following car

d_0: the minimum safe rear-to-end distance after an emergency braking event

v_f: maximum or free-flow driving speed

$x_n(t)$ and $x_{n-1}(t)$: the position of following and lead vehicles, respectively, at a given time t

S_n: distance headway between the positions of leading and following vehicles

v_n: speed of the vehicle n

a_n: the deceleration rate of vehicle n

$I_n(t)$: time headway between n^{th} and $(n-1)^{th}$ vehicles

τ_{PR}: perception-response time (PRT)

τ_n: slope in a linear spacing-speed function

τ_B: redundant time buffer used in linear car following model for autonomous vehicles

k_{jam}: jam density

w_b: backward wave speed.

To clearly examine the perception-reaction and collision-avoidance mechanism for AVs, we first briefly review the related first-order car following models. Focusing on the time dimension in the car following behavior, Forbes' model [13, 14] considers two major

elements: (i) the reaction time (e.g., 1.5 seconds) needed for human drivers to perceive the need to decelerate and apply the brakes; and (ii) the time duration for the following vehicle traversing its length (to avoid collision). Eq. (2.1) shows the equivalent distance headway.

$$d_n = 1.5v_n + L \quad (2.1)$$

In our research, using the human-driver car following behavior as the baseline, we are interested in how to adopt a linear car following model to approximate the time-continuous AV trajectories while maintaining the minimum safe driving distances. In the original classical paper by Newell [17], he derived the linear car following model as an approximation of high-order trajectories (through the mean-value theorem), while our focuses below are on how the underlying AV collision-avoidance behavior leads to space-time relationship between a pair of leading and following vehicles, as the collision-avoidance constraint between a pair of vehicles is a building block of the proposed optimization models.

First, we need to compute the minimum safety distance S_n based on the driving speed of both cars (namely v_{n-1} and v_n) before the emergency braking. The process of one leading vehicle $n-1$ and one following vehicle n under emergency braking condition is illustrated in Figure 2.1.

Step 1: Before the braking event, the minimum safety distance is S_n.

Step 2: The leading vehicle $n-1$ brakes from position B to position E;

Step 3: The following vehicle n may take a time interval of τ_n to detect the emergency braking event of the leading vehicle, and start braking from the current driving speed v_n. The following vehicle then brakes from positon A to position C.

Step 4: The minimum safe spacing after both cars stop is d_n between position C and E, that is, $d_n = d'_n + L$, where a vehicle length is L denoted by the distance between positions D and E; d'_n is the head-to-tail distance between positions C and D.

Given the deceleration rates a_{n-1} and a_n, it is easy to derive the braking distances $l = S_n + \frac{v_{n-1}^2}{2a_{n-1}}$ and $l' = v_n \times \tau_n + \frac{v_n^2}{2a_n}$ and then establish Eq. (2.2) between S_n and d_n.

$$d_n = l - l' = S_n + \frac{v_{n-1}^2}{2a_{n-1}} - v_n \times \tau_n - \frac{v_n^2}{2a_n} \quad (2.2)$$

which can be rewritten as

$$d_n = S_n - v_n \times \tau_n + \frac{v_{n-1}^2}{2a_{n-1}} - \frac{v_n^2}{2a_n} \quad (2.3)$$

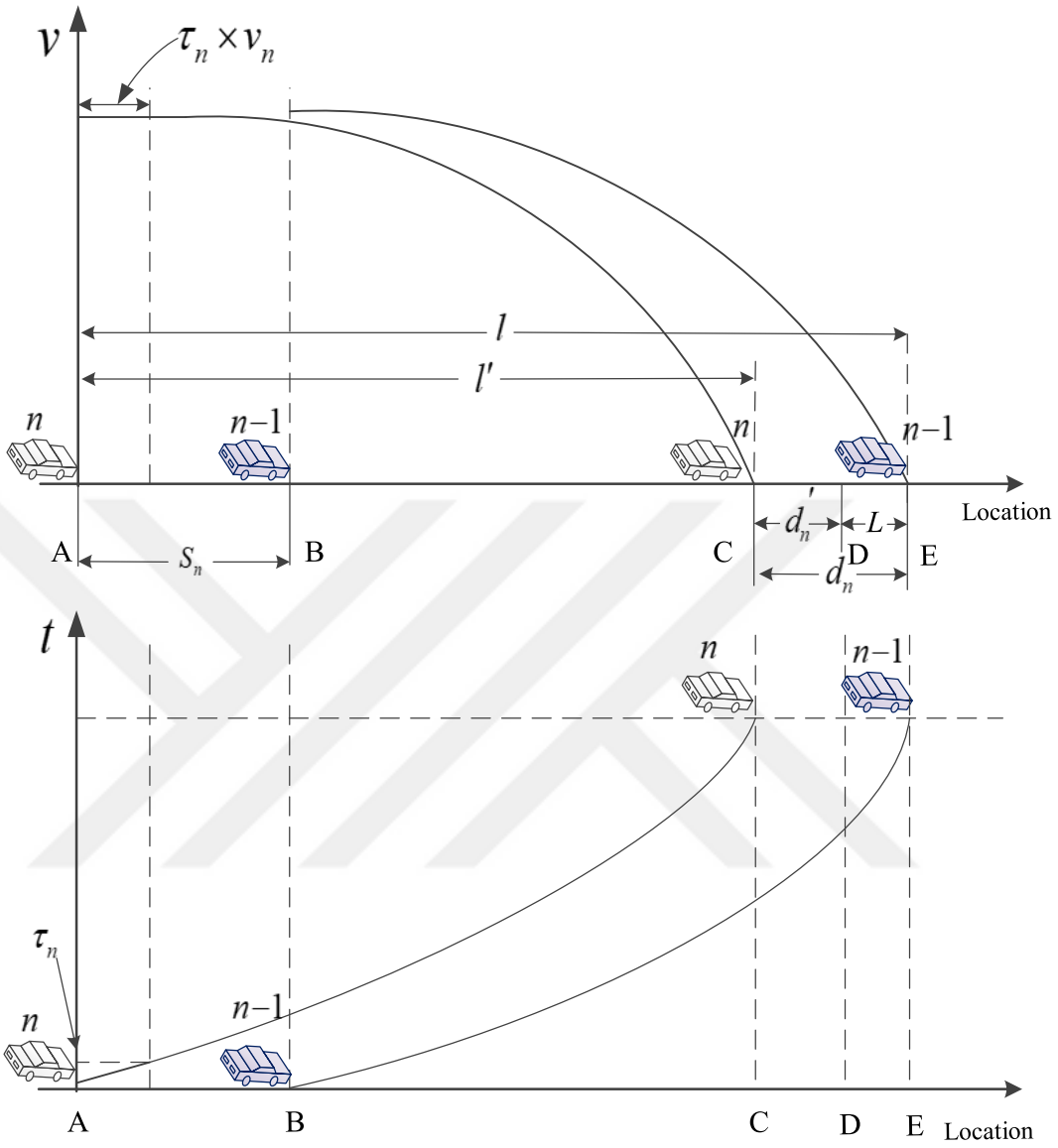


Figure 2.1 The process of car-following behavior change

Since the following vehicle is tightly following the lead vehicle, we can assume $a_{n-1} = a_n$ and $v_{n-1} = v_n$ for the same or similar type of vehicles at the stable condition. In other words, our derivation focuses more on the stable states before and after the speed changes (state transition), so one can obtain Eq.(2.4).

$$S_n = \tau_n v_n + d_n \quad (2.4)$$

Eq. (4) is consistent with Newell's simplified car-following model that distance headway S_n changes linearly with speed v_n, where τ_n and d_n are independent of its vehicle speed

v_n . The relation between spacing S_n and velocity v_n and the simplified car-following trajectory is shown in Figure 2.2.

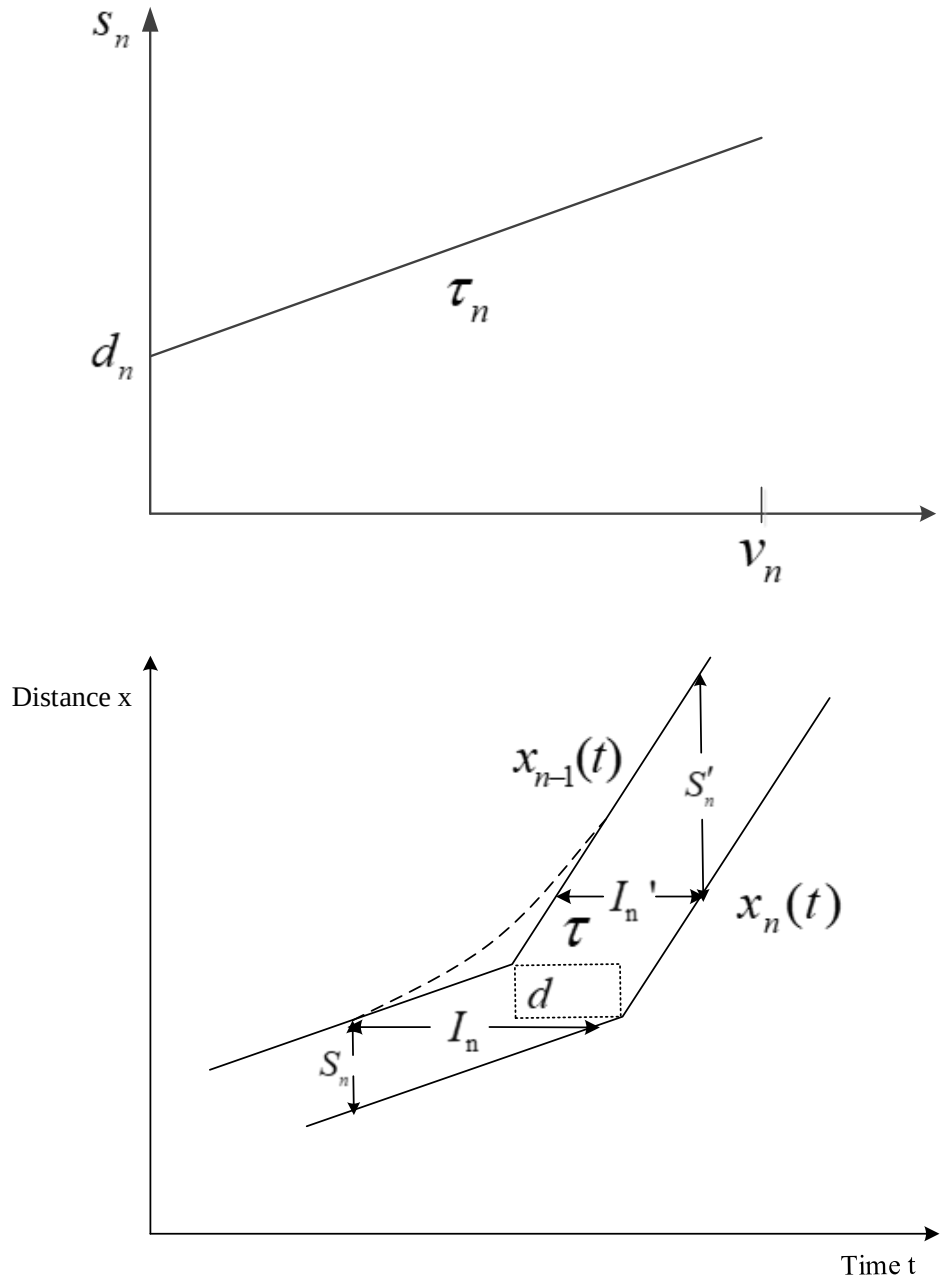


Figure 2.2 Relation between spacing and velocity and piecewise linear approximation to vehicle trajectories with a speed change (adapted from Newell [17])

Now we discuss possible values of perception and reaction time parameter τ_n under different cases.

If the lead car is human operated (but possibly connected) and the following one is an automated car, τ_n should include a detection delay (about 0.3s) and emergency braking delay (about 0.4s), as shown by Ioannou et al [68].

If both vehicles are AVs and their driving speed information is completely shared in real time, τ_n can be significantly small as 0. This implies that $S_n = d_n$. This case applies to the AVs among an AV platoon.

To reduce the unexpected secondary accident impact, and to ensure the overall system reliability and stability, in the AHS designed by Varaiya [6] and Bose and loannou [69], an extra distance buffer $v_n \times \tau_B$ is given as shown in Eq. (2.5).

$$S_n = v_n \times \tau_{PR} + v_n \times \tau_B + d_n \tag{2.5}$$

where $\tau_{PR} + \tau_B$ in Eq. (5) is the desired time headway of autonomous vehicles, defined as the time taken to cover the distance $S_n - d_n$. Within a speed-spacing relationship described in Eq. (4), a unified formula for the slope parameter τ_n can be represented as $\tau_n = \tau_P + \tau_R + \tau_B$, where τ_P and τ_R are the corresponding perception and reaction time and $T_{PR} = \tau_P + \tau_R$.

Table 2.1 further examines the differences of the above mentioned car-following models in both human operated and autonomous vehicles.

Table 2.1 Different interpretations of linear car following model $S_n = \tau_n \times v_n + d_n$ with sample settings

Model	Time Offset τ_n			Distance offset
	Perception time	Response time	Redundant time buffer	
Newell's Model (human operated cars)	1-1.3	0.4	Not defined	d_n
Automated and connected car model	Very small, related to communication delay	Very small, related to machine and vehicle processing time	τ_B	d_n

In this section, we are interested in deriving the corresponding macroscopic flow-speed or flow-density relationship based on the proposed microscopic AV driving behavior, like given τ_k and d_k. As shown in Figure 2, based on Eq. (4), we can derive the time headway $I_n(t)$ between n^{th} and $(n-1)^{th}$ vehicles as shown in Eq. (2.6),

$$I_n = \frac{S_n}{v_n(t)} = \frac{\tau_n \times v_n(t) + d_n}{v_n(t)} = \tau_n + \frac{d_n}{v_n(t)} \tag{2.6}$$

So the general time headway can be as, $\bar{I} = \bar{\tau} + \frac{\bar{d}}{v}$, where $\bar{\tau} = \frac{1}{n}\sum_{k=1}^{n} \tau_k$ and $\bar{d} = \frac{1}{n}\sum_{k=1}^{n} d_k$

Since the flow rate q can be expressed as $q = \frac{1}{\bar{I}}$, the capacity (maximum flow rate) is derived when speed reaches the maximum speed, free-flow speed v_{max}.

$$q_{max} = 1/(\bar{\tau} + \frac{\bar{d}}{v_{max}}) \tag{2.7}$$

Where jam density $k_{jam} = \frac{1}{\bar{d}}$, and backwave speed

$$w_b = \frac{q_{max} - 0}{k_{jam} - k_c} = \frac{\bar{d}}{\bar{\tau}}. \tag{2.8}$$

Eqs. (7) and (8) have been shown as a critical bridge between Newell's microscopic car-following model and macroscopic flow-density fundamental triangle diagram, and many studies (e.g., [17]) have used a similar form to quantify the capacity impact under a connected or automated vehicle environment under different driving conditions.

2.2 Model leader-follower behavior in multi-AV formation control with changeable reaction times

As shown in the right plot of Figure 2.3, before the speed changes from v_1, one can show that, $s_n = \tau_n \times v_1 + d_n$. If the velocity changes to v_2 , similarly, it can obtain $s_n' = \tau_n \times v_2 + d_n$. Assuming that the following vehicle n is tightly following the lead vehicle $n-1$, it is obvious that $x_{n-1}(t) - x_n(t+\tau_n) = S_n - \tau_n \times v_1 = d_n$ and $x_{n-1}(t) - x_n(t+\tau_n) = S_n' - \tau_n \times v_2 = d_n$. Thus we can further derive the car-following constraints in the time and space dimension, before and after speed changes.

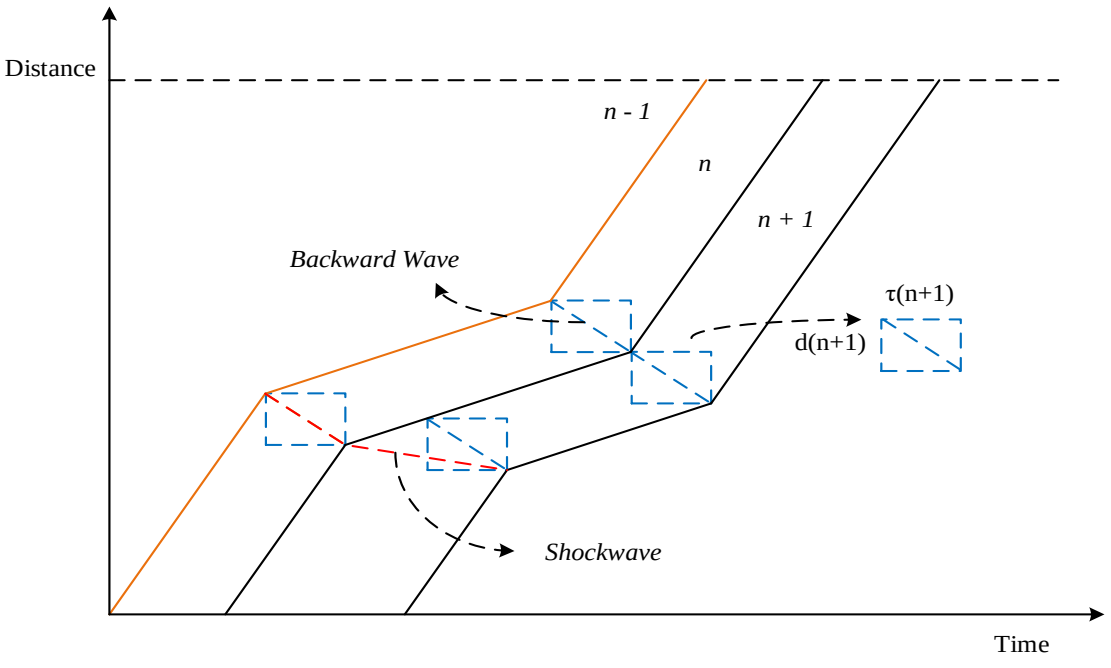


Figure 2. 3 Vehicles' trajectory based on simplified car following model

$$x_n(t + \tau_n) = x_{n-1}(t) - d_n \quad (2.9)$$

By considering both free-flow and car following mode, we can obtain an inequality constraint in Eq. (2.10) shown by Newell [17] as shown in Figure 2.3.

$$x_n(t + \tau_n) = \min\{x_n(t) + v_f \times \tau_n, x_{n-1}(t) - d_n\} \quad (2.10)$$

If we extend Eq. (10) to another following vehicle n + m recursively, one can easily derive

$$x_n(t + \sum_{i=n}^{n+m} \tau_i) = \min\{x_{n+m}(t) + v_f \times (\sum_{i=n}^{n+m} \tau_i), x_{n-1}(t) - \sum_{i=n}^{n+m} d_i\} \quad (2.11)$$

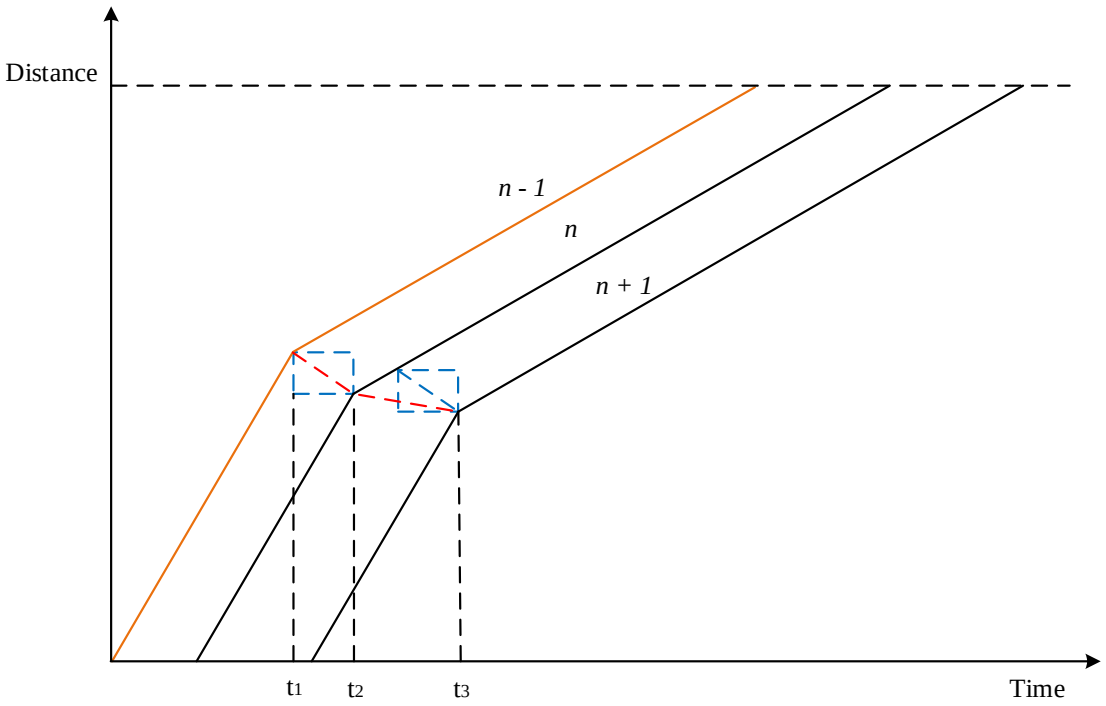


Figure 2. 4 Vehicles' trajectory from free flow speed to congested speed

Now, to better control the multi-robot trajectory, we consider a leader-follower formation control approach with dynamically changing reaction times, which is motivated by two reasons: (i) it is still a challenge to fully control each individual autonomous vehicle in a large scale, and (ii) a changeable reaction time (which is greater than the minimum reaction time) can reduce the collision risk, to some extent. The details will be discussed later.

Trajectories of a platoon consisting of 5 AVs are shown in Figure 2.6. with constant reaction time and variable speed 30 mph to 60 mph. As shown in Eq. (6) or (7), capacity or time headway consumed by a set of vehicles, is dependent on two factors: reaction time and speed. By reducing or dynamically changing the reaction time during the journey of a multi-vehicle moving process, as illustrated in Figure 2.7, we can increase the

capacity throughput at the critical bottleneck as shown in Figure 2.9 and Figure 2.10 where the speed is 30 mph.

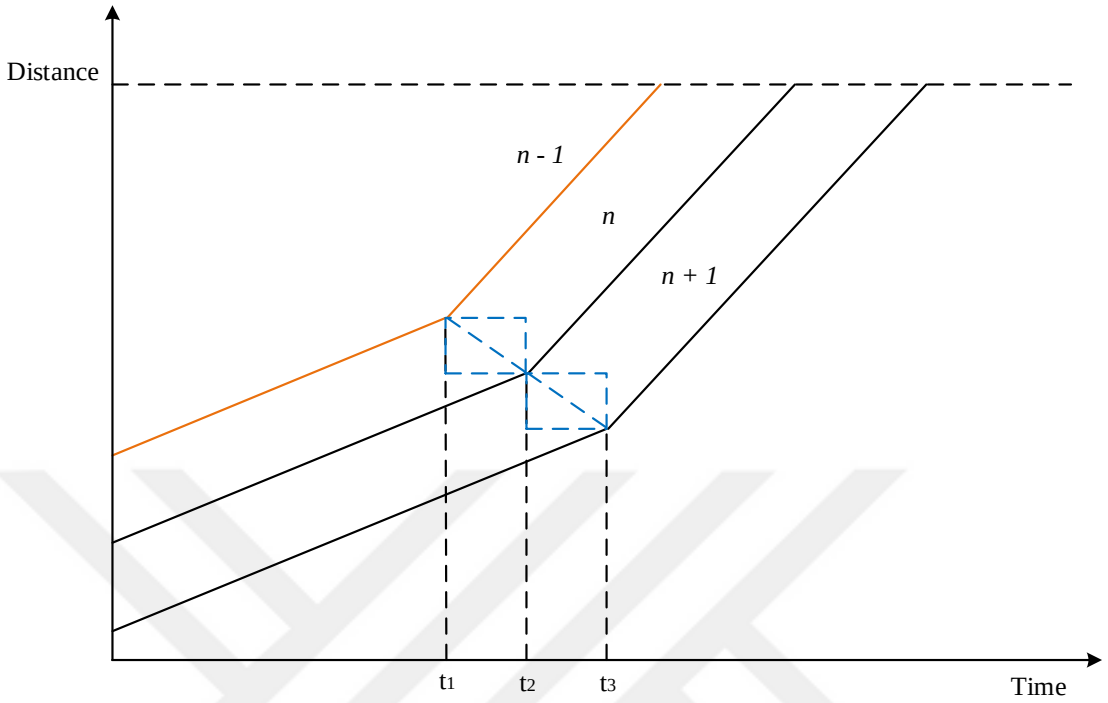


Figure 2. 5 Vehicles' trajectory from congested speed to free-flow speed

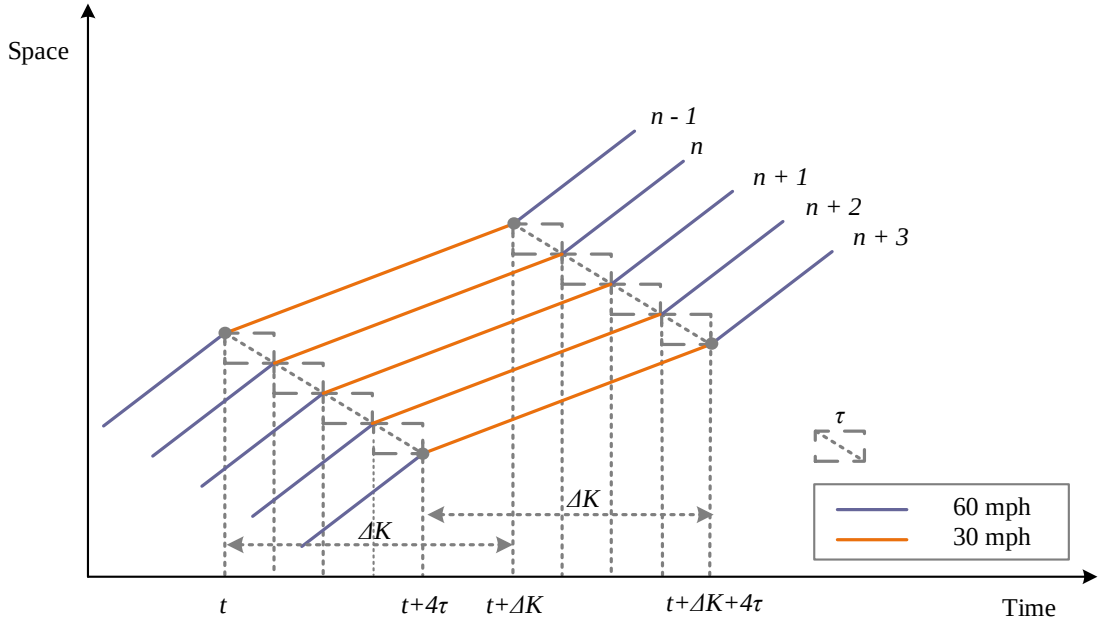


Figure 2. 6 Constant reaction time, speed is changing from 60 mph to 30 mph and from 30 mph to 60 mph

All AVs in the platoon can pass the bottleneck without any splitting when the reaction time is 0 s in Figure 2.9 and Figure 2.10. To show the effectiveness of changing reaction times, possible trajectories of AVs with regular reaction time, $\tau_1 = 1.5\ s$, are plotted as

green dashed lines at the critical bottleneck. As can be seen in Figure 2.9 and Figure 2.10, if the reaction time didn't change, not all AVs in the platoon could pass the bottleneck without splitting. That is, 2 vehicles in Figure 2.9 and Figure 2.10 are left behind the green time interval.

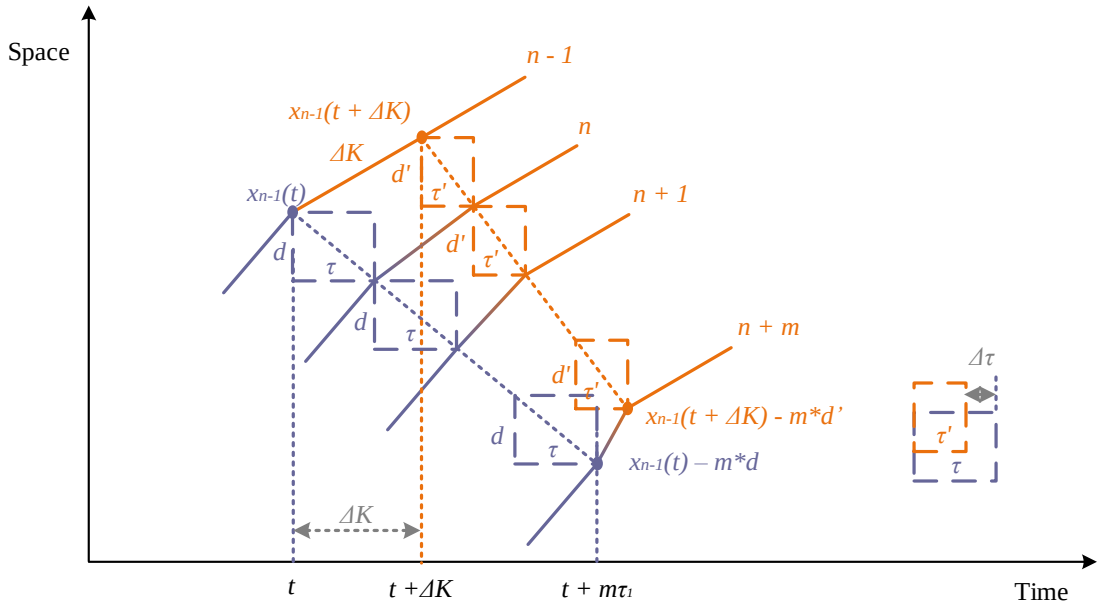


Figure 2. 7 Reaction time changing constraints

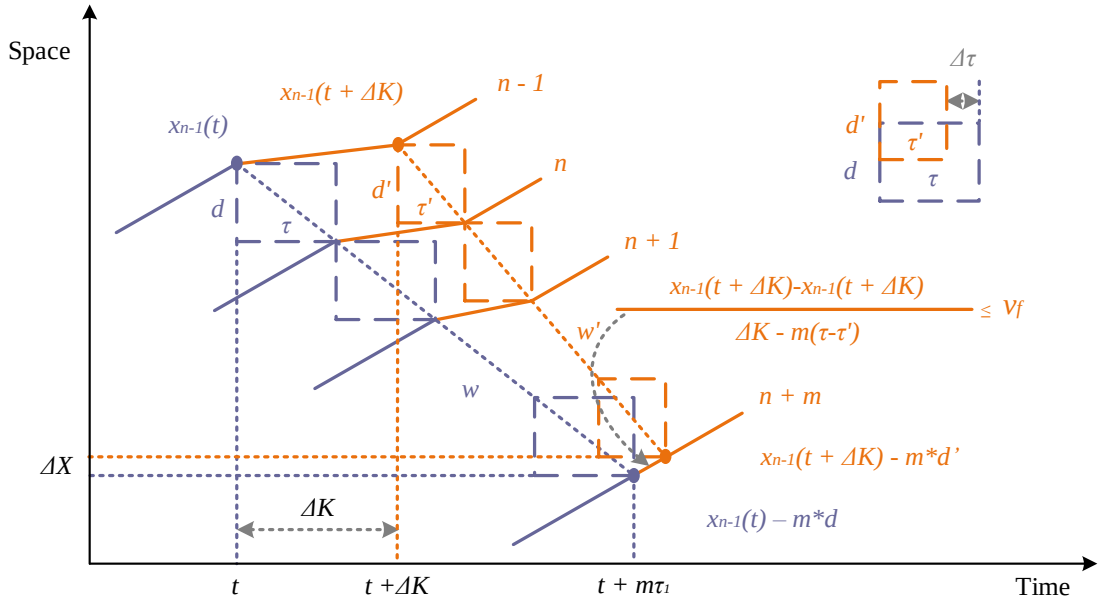


Figure 2. 8 Speed limit for transition process

When we are able to adjust the variable reaction time between two optimization time steps, we need to carefully consider a special constraint to ensure the follower still moves forward as a result of two backward wave propagations. As shown in Figure 2.7, after

changing the reaction time, the new timestamp of the follower must be greater than the previous timestamp, which leads to Eq. (2.12).

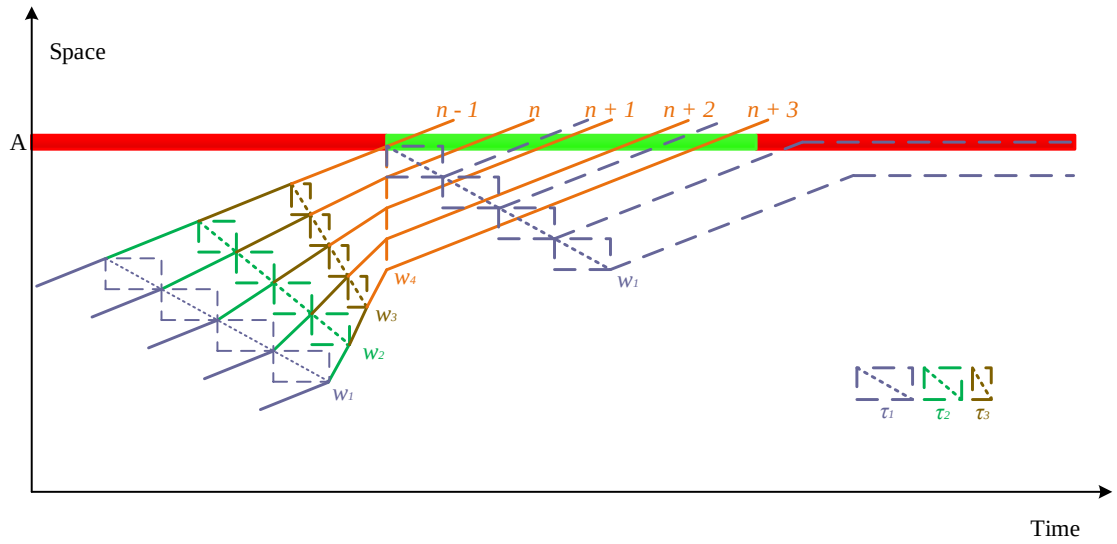


Figure 2. 9 Reaction time is changing with $\tau 1$ = 1.5 s, $\tau 2$ = 1 s, $\tau 3$ = 0.5 s, $\tau 4$ = 0 s without defining speed limit

$$t + \Delta K + m * \tau' > t + m * \tau \quad (2.12)$$

where ΔK is time difference between timestamps of reaction time change events, τ is the previous reaction time, τ' is current reduced reaction time. Assuming ΔK as 1 time interval, we can rewrite constraint (12) as $t + 1 + m * \tau' > t + m * \tau$, which leads to

$$(\tau - \tau') < \frac{1}{m} \quad (2.13)$$

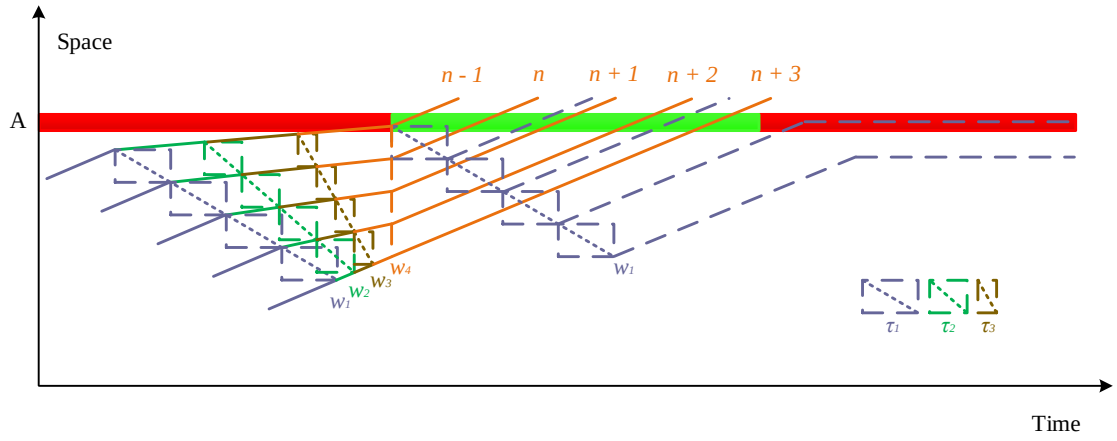


Figure 2. 10 Reaction time is changing with $\tau 1$ = 1.5 s, $\tau 2$ = 1 s, $\tau 3$ = 0.5 s, $\tau 4$ = 0 s with defining speed limit

That is, the magnitude of reaction time change $\Delta\tau$ must be less then $\frac{1}{m}$. After changing the reaction time, we need to ensure that the vehicle is not moving backward. That is, the new position of the followers must be larger than their previous position:

$$x_{n-1}(t+\Delta K) - m * d' \geq x_{n-1}(t) - m * d \quad (2.14)$$

where d and d' are the previous and current minimum distance between leading and following cars, respectively. For simplicity, if we assume d and d' have the same value, inequality (14) always holds.

It should be noted that in the transition process above, it is possible that the following vehicle(s) could have a short time period where the prevailing speed could temporally exceed the speed limit. For example, the lead vehicle is driving at the speed limit and the following vehicles need to catch up and form the platoon. This is the by-product of variable reaction times. To mitigate this issue, one could either reduce the speed of the lead vehicle to allow the following vehicles to catch up under the speed limit requirement, or expand the transition duration for variable reaction time so we have a smoother transition to reduce the possibility of temporally violating speed limit for the following cars.

To satisfy speed limits for all vehicles, it has to be define new constraint in the course of reaction time changing while vehicles are coupling. As shown in Figure 2.8, while the last following vehicle keeps its speed, the leading vehicle should slow down. For the last vehicle: $\Delta X = (x_{n-1}(t+\Delta K) - m * d') - (x_{n-1}(t) - m * d)$. Since $d = d', \Delta X = x_{n-1}(t+\Delta K) - x_{n-1}(t)$. For the last vehicle: $\Delta T = (t + \Delta K + m * \tau') - (t + m * \tau)$, which leads to $\Delta t = \Delta K - m(\tau - \tau')$. Therefore, if the last vehicle cannot have a speed greater than speed limit, $\frac{\Delta X}{\Delta T} \leq v_f$. Thus we can further derive the speed limit constraint for changing reaction time.

$$\frac{x_{n-1}(t+\Delta K) - x_{n-1}(t)}{\Delta K - m(\tau - \tau')} \leq v_f \quad (2.15)$$

2.3 Probability density function (PDF) of communication delay and its impact on driving risk

In general, a cooperative driving environment is expected to provide significant improvements for road safety and traffic flow efficiency [70, 71, 72]. Before presenting further analytical results, we now briefly review the related studies for measuring the impact of communication delay in different vehicular communication environments. Bai

and Krishnan V2V reliability in the application level, as a function of (i) distance headways between successive following vehicles and (ii) tolerance time window [73]. According to their experimental results based on different distance headway from 25 m up to 400 m, packet delivery ratio, a common metric in the literature, is changing between 93% and 58%, respectively. Many studies, such as Xu et al., focused on quantitative characterization of the communication latency in a platoon, dependent on communication structures and content as well as communication standards [74]. Cheng et al. (2017) proposed a 5G-enabled cooperative intelligent vehicular (5GenCIV) framework to provide secure autonomous driving by enabling ultra-low latency typically requiring a time delay in the scale of microseconds, which could enable higher speed and lower space in the CAV environment discussed in our paper [75].

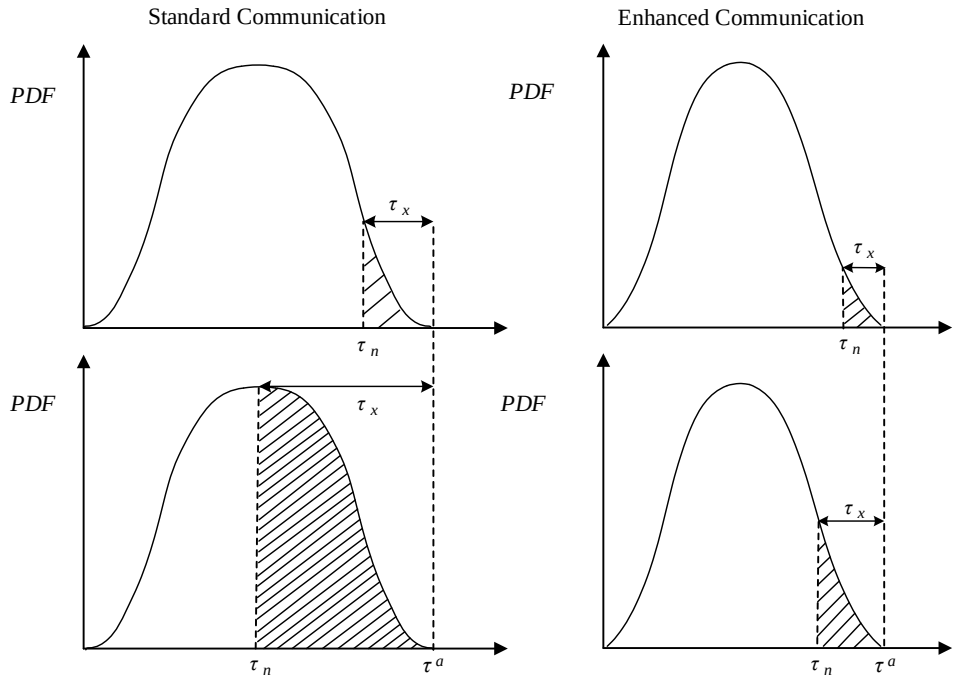


Figure 2. 11 PDF of reaction times

With changeable reaction time, we not only need to precisely compute the benefit of increased capacity, but also estimate the associated risk due to reduced reaction time threshold, as shown in the probability density function (PDF) of communication delay in Figure 2.11. τ_n is a team-based reaction time threshold agreed upon by each vehicle in the platoon. τ_x is the extra communication delay (due to transmission error of data) beyond τ_n, and τ^a is the actual combined time delay as the summation of τ_n and τ_x. The magnitude of τ_x depends on the specific communication system used. As Figure 2.11 shows, τ_x is greater under a standard communication system (e.g. DSRC) than under

enhanced communication system (e.g. 5G). In a perfect car following behavior, the following vehicle should start to slow down at time $t + \tau_n$, , and starts emergency braking at time $t + \tau^a$. For a given extra delay τ_x, the braking time is $\Delta t_{TC} = \frac{v_n - v_{n-1}}{a_n}$ and the braking distance is $\Delta x_{TC} = \frac{v_n^2 - v_{n-1}^2}{2a_n}$., as illustrated by the space-time diagram shown in Figure 2.12.

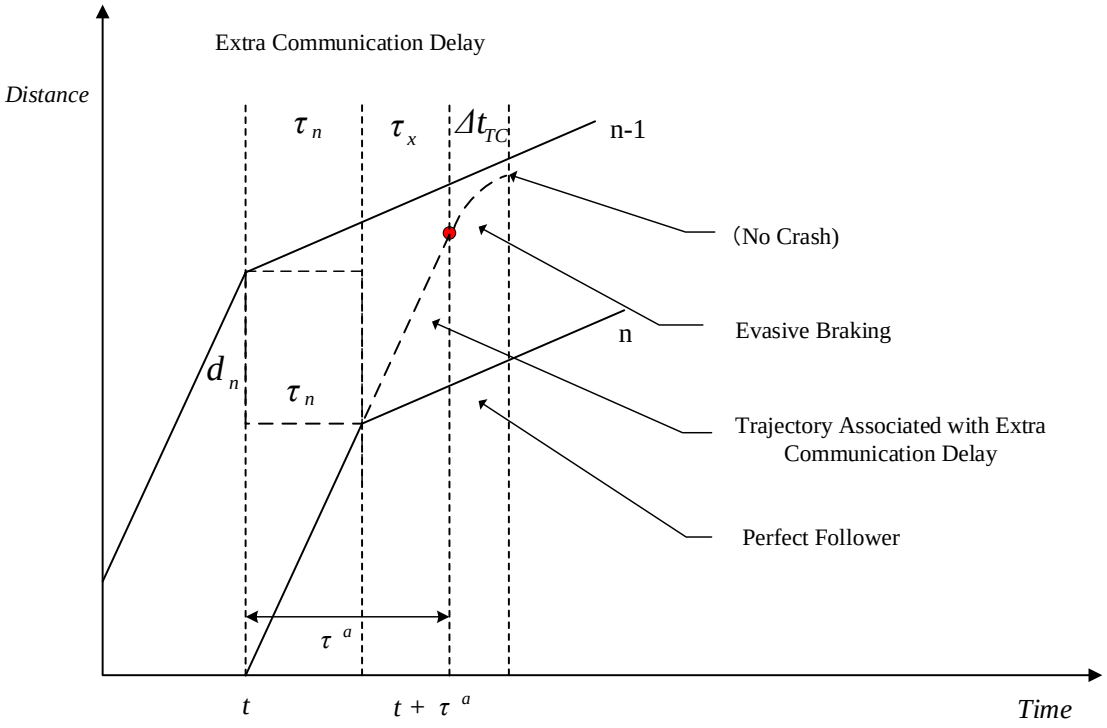


Figure 2. 12 Relation between spatial distance and time considering response time lag (adapted from [66]).

In order to guarantee the leading and following vehicles (X_{n-1}^a and X_n^a) do not collide, the position relationship between them at time ($t + \tau^a + \Delta t_{TC}$) should meet the following inequality constraint.

$$X_{n-1}^a(t + \tau^a + \Delta t_{TC}) \geq X_n^a(t + \tau^a + \Delta t_{TC}) + L \quad (2.16)$$

Following the derivation step by Przybyla et al., [66] for distracted driving, at time ($t + \tau^a + \Delta t_{TC}$), the position of the leading and following vehicle could be represented as

$$X_{n-1}^a(t + \tau^a + \Delta t_{TC}) = v_{n-1} \times (\tau^a + \Delta t_{TC}) + X_{n-1}^a(t) \quad (2.17)$$

$$X_n^a(t + \tau^a + \Delta t_{TC}) = X_{n-1}^a(t) - d_n - \tau_n * v_n + v_n \times \tau^a + \Delta x_{TC} \quad (2.18)$$

Using the Eqs. (16) and (17), the probability of success equals to

$$P_{s_n} = Prob(X_{n-1}^a(t + \tau^a + \Delta t_{TC}) > X_n^a(t + \tau^a + \Delta t_{TC})) \quad (2.19)$$

It should be noted that the probability of success depends on the distribution of actual communication delay τ^a, and the preset response time value τ_n for given speed and positions of two vehicles. The team-based risk probability for m vehicles in the platoon can be calculated as follows

$$R_c = 1 - \prod_{n=1}^{m} P_{s_n} \quad (2.20)$$

As a remark, traffic boundary condition (closed or semi-open) is an important input for autonomous vehicle trajectory control/optimization. Our proposed model can handle not only the closed boundary condition in the space-time network but also the semi-open boundary condition through building a virtual super-destination node with the objective of travel time, fuel consumption, emissions, etc.

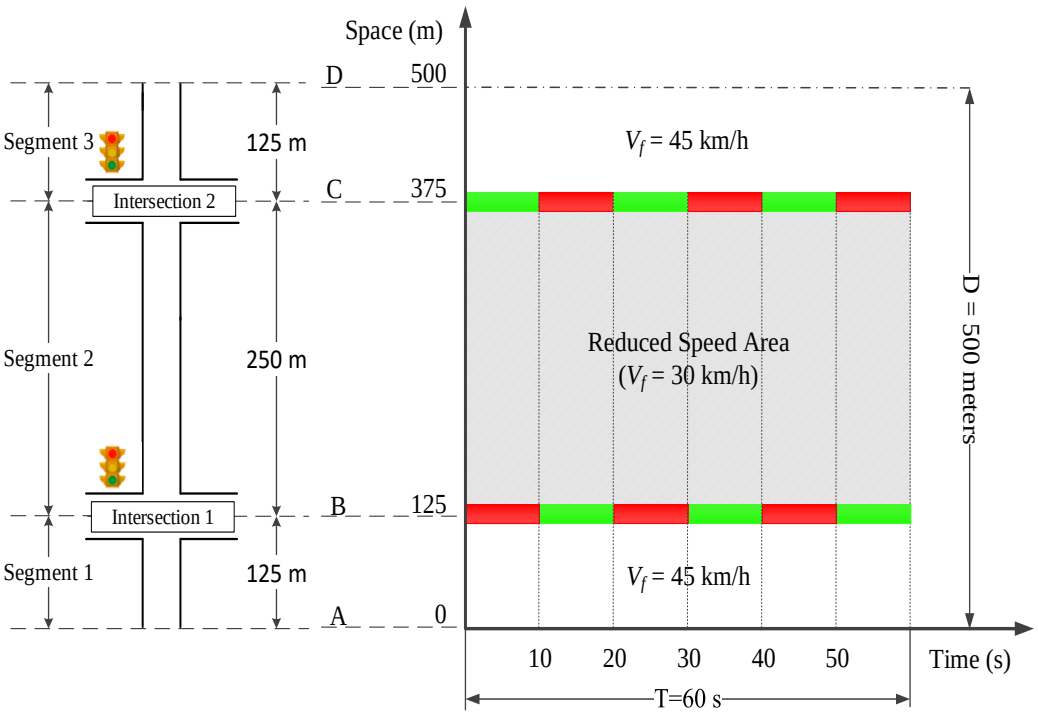
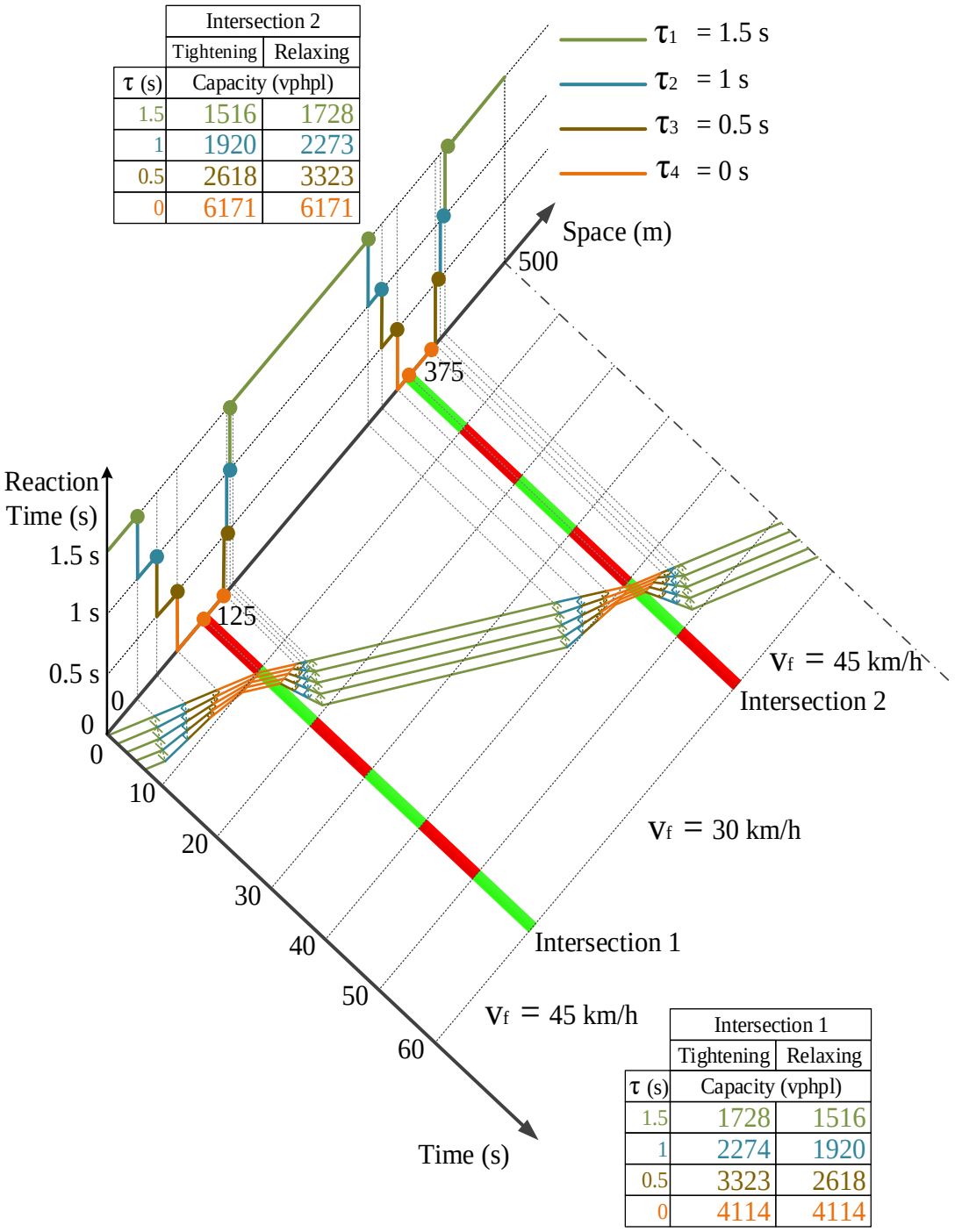


Figure 2. 13 Layout of hypothetical road segment of space and time axes for 3D illustration of trajectories.

Figure 2. 13 gives the layout of hypothetical road segment of space and time axes for 3D illustration of trajectories. Figure 2.14 illustrates in three dimensions (reaction time, space, and time) how reducing reaction times in follower vehicles increases capacity throughput at signalized intersections. The trajectories of the lead vehicle and four following vehicles are analyzed along a three-segment roadway with two traffic signals under three free flow speeds at different segments and four reaction times. Four different

colors representing four changing reaction times (green for 1.5 s, blue for 1.0 s, brown for 0.5 s, and orange for 0 s).



	Intersection 2	
	Tightening	Relaxing
τ (s)	Capacity (vphpl)	
1.5	1516	1728
1	1920	2273
0.5	2618	3323
0	6171	6171

	Intersection 1	
	Tightening	Relaxing
τ (s)	Capacity (vphpl)	
1.5	1728	1516
1	2274	1920
0.5	3323	2618
0	4114	4114

Figure 2.14 3D illustration of trajectories of AVs' and reaction time changing at the critical bottlenecks

In order to achieve a tightly coupled platoon with zero or closer-to-zero reaction time, as shown at intersections in Figure 2.14 and Table 2.2, this requires a future generation of communication standard with maximum service rate (MSR) of 4114 vehicles per hour per lane (vphpl) at intersection 1 and 6171 vphpl at intersection 2 for speeds of 30 km/h and 45 km/h, respectively. For a reaction time of 1.5 s, with the MSR of 1728 vphpl and 1516 vphpl for speeds of 45 km/h and 30 km/h, respectively, dedicated short range communication (DSRC) seems to be sufficient based on our very simplified analysis. More importantly, Figure 2.14 aims to shed some lights to another important research problem, namely how to optimize vehicle/platoon approaches to signals considering this potential automated vehicle condition.

Table 2.2 Service rates at the critical bottlenecks

Reaction Time	Intersection 1		Reaction Time	Intersection 2	
	Tightening	Relaxing		Tigtening	Relaxing
	Capacity (vphpl)			Capacity (vphpl)	
1.5	1516	1728	1.5	1728	1516
1	1920	2273	1	2274	1920
0.5	2618	3323	0.5	3323	2618
0	6171	6171	0	4114	4114

Specifically, we should note that the proposed model does assume the reaction time is controllable and its minimum reaction requirement is determined by the communication environment or the nature of the communication facilities. What is more, the result of controllable reaction time on following vehicles is our desired speed change or trajectory control for platoon formation under acceptable collision risks. In some cases, permitting the reaction time equal to 0 may cause traffic safety issue, while our examples could be easily re-implemented using a more realistic but small value like 0.1s or 0.5 s.

CHAPTER 3

DYNAMIC PROGRAMMING FOR MULTIPLE VEHICLE TRAJECTORY OPTIMIZATION WITH CHANGEABLE REACTION TIMES IN A PLATOON

3.1 An overview of Dynamic Programming

Dynamic Programming was introduced in the 1950's by using Bellman's Principle of Optimality ([76]). According to the Bellman optimal policy was defined as below:

> "An optimal policy has the property that whatever the initial state and initial decision are, the remaining decisions must constitute an optimal policy with regard to the state resulting from the first decision."

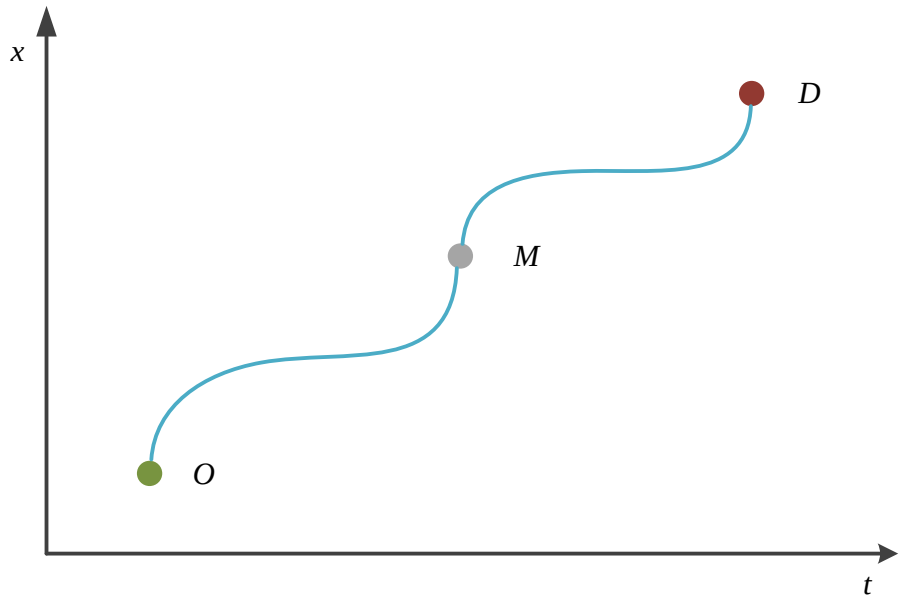


Figure 3.1 Principle of optimality; as M is on the optimal path from O to D, the optimal path from M to D is what remains of the same path. *t* is time and *x* is the state of the system

The Principle of Optimality defines an optimal path from O to D with the new point M as shown in Figure 3.1. The main use of the Principle of Optimality is that if we know all optimal paths for any initial state x at time $n + 1$, then every optimal path starting at time n must use one of these optimal paths from time $n + 1$ and for continued steps as shown in Figure 3.2.

3.1.1 Mathematical Formulation

We can introduce some mathematical equations for next levels. We should define the notation used in this section as further. We let the state of our system be denoted x. This is usually a finite dimensional vector of real numbers, and it's dimension was defined 1 in the illustrations 1 for simplicity (i.e. x is a number). Time can be evolved in discretely as illustrated in Figure 3.2. At time n with a state of $x(n)$, the controller has to choose a control action $u(n)$ that brings the system to state $x(n + 1)$ at time $n + 1$ according to the system dynamics $f(x, u)$:

$$x(n + 1) = f(x(n), u(n)) \tag{3.1}$$

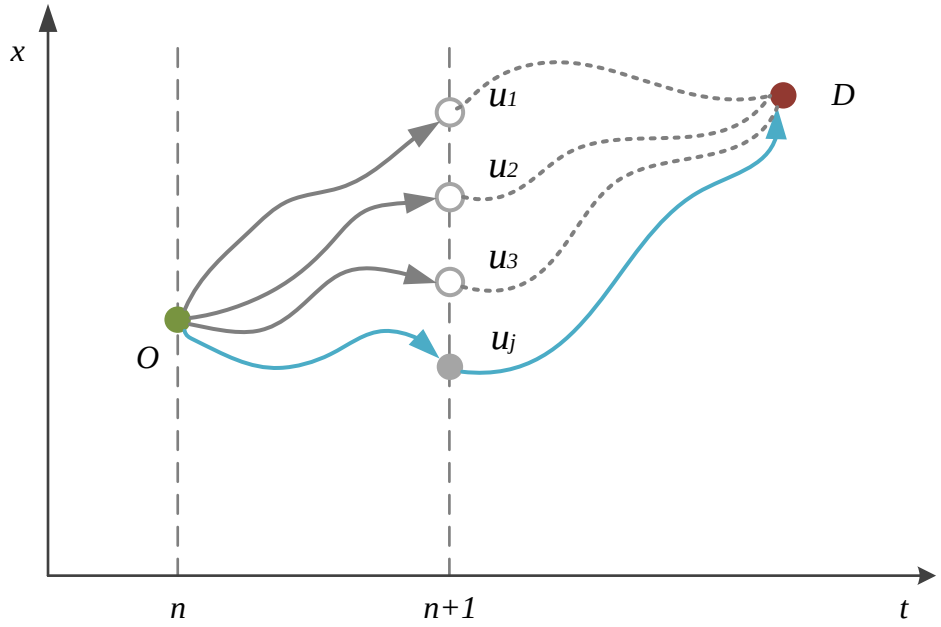


Figure 3.2 Different paths from *O* to *D*, and the actions u_j is optimal path from *O* to *D*.

If we discuss optimality of certain paths and control actions, we have to introduce a notion of cost. An optimal path is a path from an initial state $x(n)$ which minimizes some cost J. In Dynamic Programming, it is used a time additive cost, which consists of a sum of step costs $l(x, u)$:

$$J\big(x(.),u(.)\big) = \sum_{n=0}^{N} l\big(x(n),u(n)\big) \quad (3.2)$$

A feedback control law

$$u(n) = \mu(x,n) \quad (3.3)$$

assigns an action for any time *n* and state *x*. When this control law is applied to the system, it evolves as

$$x(n+1) = f(x(n),\mu(x,n)) \quad (3.4)$$

An optimal control law $\mu^*(x,n)$ is one that minimizes the cost *J* for any initial state.

3.1.2 Optimal Control Action

After defining the optimal control law, next steps are to find it. As previously mentioned, if the optimal feedback law is known for any state x at time $n+1$, then all the controller has to decide at time n is which action to take at the first step. The total cost using the optimal control law from state x, at time $n+1$ can be defined as $V^*(x,n+1)$. This function is called as the optimal value function.

The role of the controller at time n is to choose an action u such that the sum of the step cost from n to $n+1$ and the left cost from $n+1$ is minimized. This is the principle of Bellman's equation:

$$V^*(x,n) = \min_{u(n)}\{V^*\big(f\big(x(n),u(n)\big),n+1\big) + l(x(n),u(n))\} \quad (3.5)$$

Given the value function $V^*(x,n+1)$ we can thus calculate both the value function $V^*(x,n)$ and control law $u(n) = \mu(x,n)$ at time n. Therefore, the optimal feedback control law can be found by iteration, starting at the final step and solving backwards in time called as value iteration. We note that the only data that needs to be kept between each iteration is the value function.

Another way to solve for a steady-state solution of Bellman's equation is policy iteration through the iterating the following two steps.

- Calculation of the corresponding infinite time value function $V_k(x)$ with given a steady state control law $\mu_k(x)$.
- Calculation an advanced control law $\mu_{k+1}(x)$ from a value function $V_k(x)$.

This method can give very fast convergence when we have a good control law (or initial value function).

3.2 Different models and control variables

As shown in the extended form of Newell's car following model with multiple following vehicles in Eq. (11), one can control the lead vehicle to implicitly control all following autonomous vehicles. To enable the real-time platoon formation and control, we transform the vehicle control model as a dynamic programming problem, which serves as a foundation for many vehicular movement controllers.

There are different levels of longitude vehicle trajectory control problems (with simplified car following model), as shown in Figure 9. Table 2 lists all basic elements of dynamic programming for single vehicle trajectory control (mode 1) and two coupled vehicle trajectory control (mode 1+1), 1 leader controlling tightly coupled followers (mode 1+m), and 1 leader controlling tightly coupled followers with variable backwave speed w, (mode 1+m (w)).

Table 3.1 Description of different modes

No.	Mode	Description	Control Variable
(1)	1	One single optimized autonomous vehicle	Single vehicle trajectory
(2)	1 + 1	Two jointly optimized autonomous vehicles (the second vehicle is not necessary at a following mode)	Trajectories of leader and follower
(3)	1 + m	One optimized lead AV and m following vehicles with fixed reaction time	Trajectory of leader
(4)	1 + m(w)	One optimized lead AV and m following vehicles with variable reaction time	Trajectory of leader and (variable) platoon-level reaction time along backward wave line

In Figures 3.3, 3.4, 3.5 and 3.6, the discretized time unit is one-time interval, and the discretized space unit is also defined on the basis of feasible vehicle speeds, which have three alternatives from 0 to the maximum speed limit for constraint (10). Assume that the optimized vehicle trajectory has been found through dynamic programming as shown in Figures 3.3, 3.4, 3.5 and 3.6. The green trajectory is for the lead vehicle and the orange trajectory is for following vehicles. The dashed lines are the backward wave for the tight

car following condition. The backward wave speed is equal to d/τ based on equation (8). The solid red trajectory represents the safety boundary of the lead vehicle that all following vehicles cannot enter in Figure3.4.

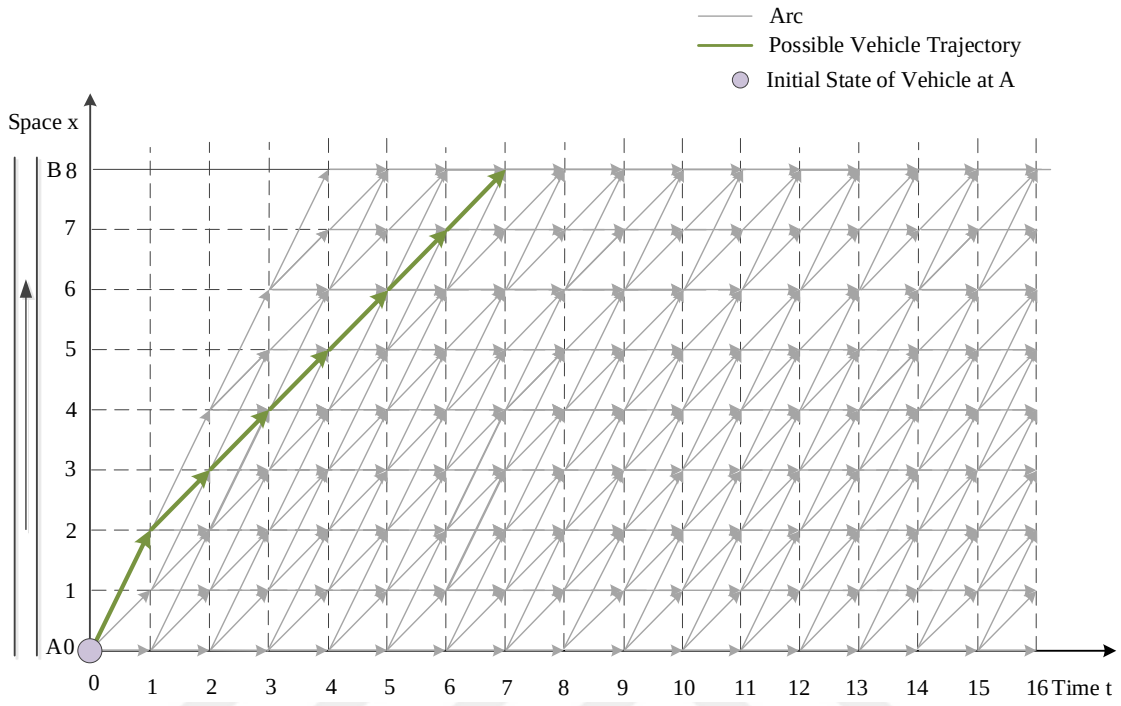


Figure 3.3 Discretized space-time network for vehicle trajectory optimization for (1)

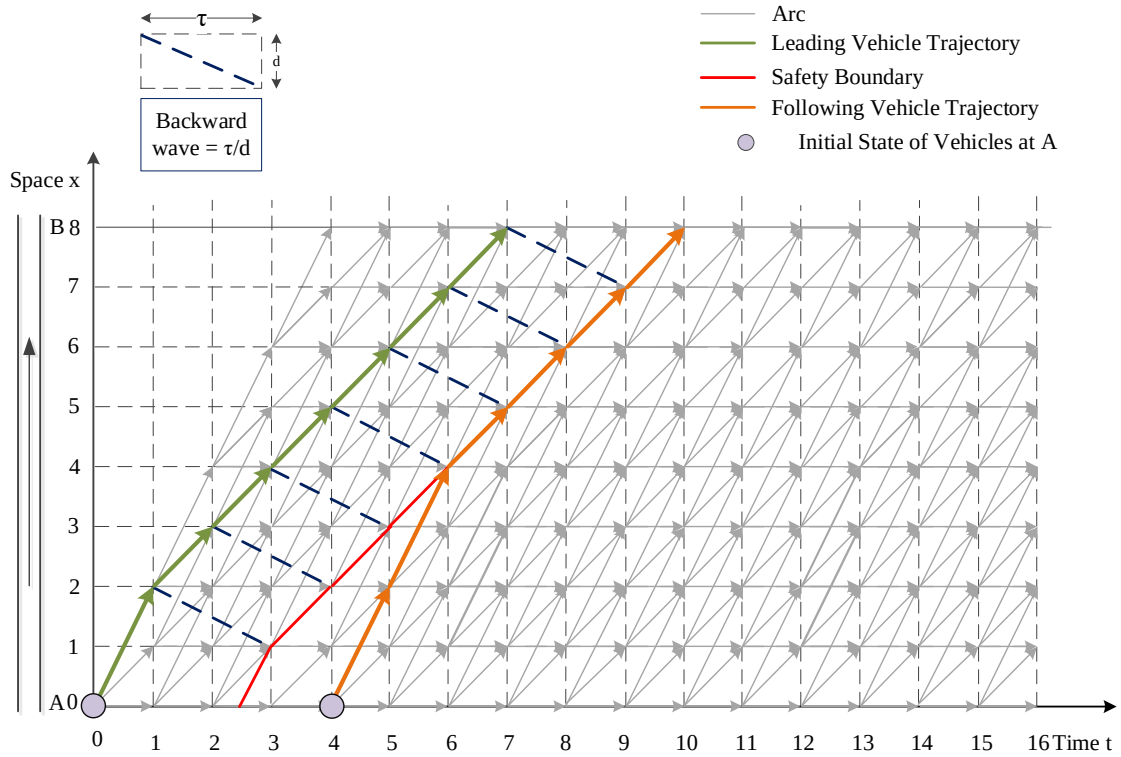


Figure 3.4 Discretized space-time network for vehicle trajectory optimization for (1+1)

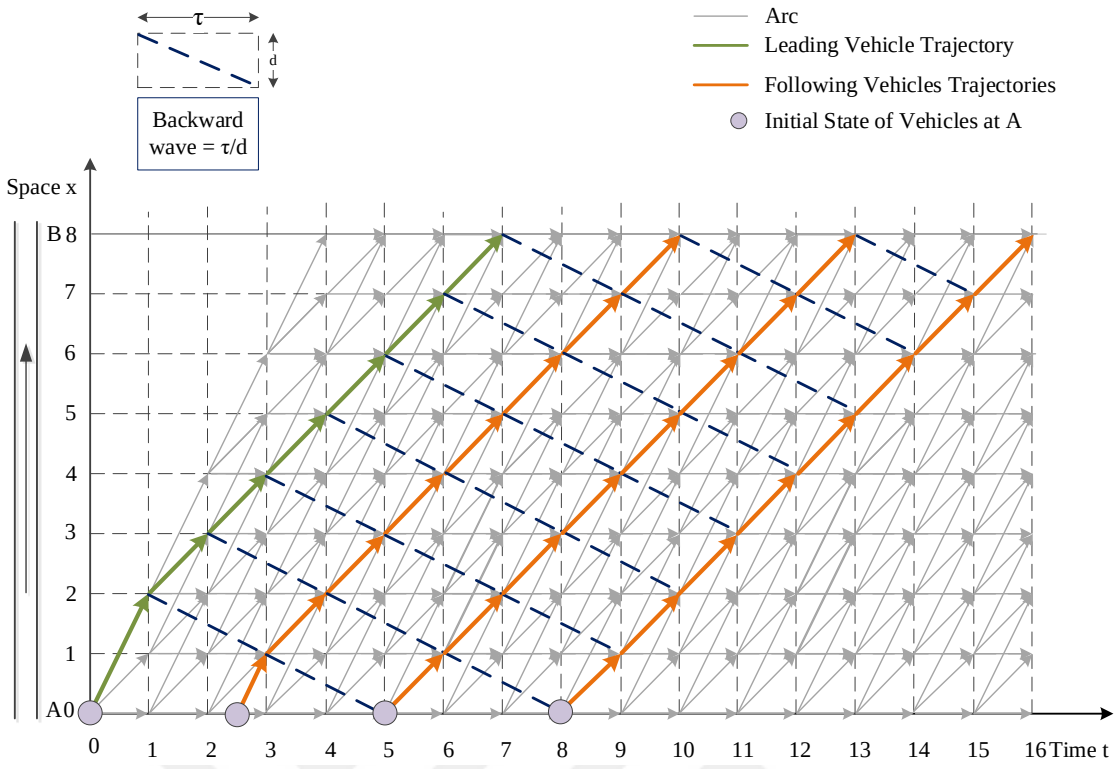


Figure 3.5 Discretized space-time network for vehicle trajectory optimization for (1+m)

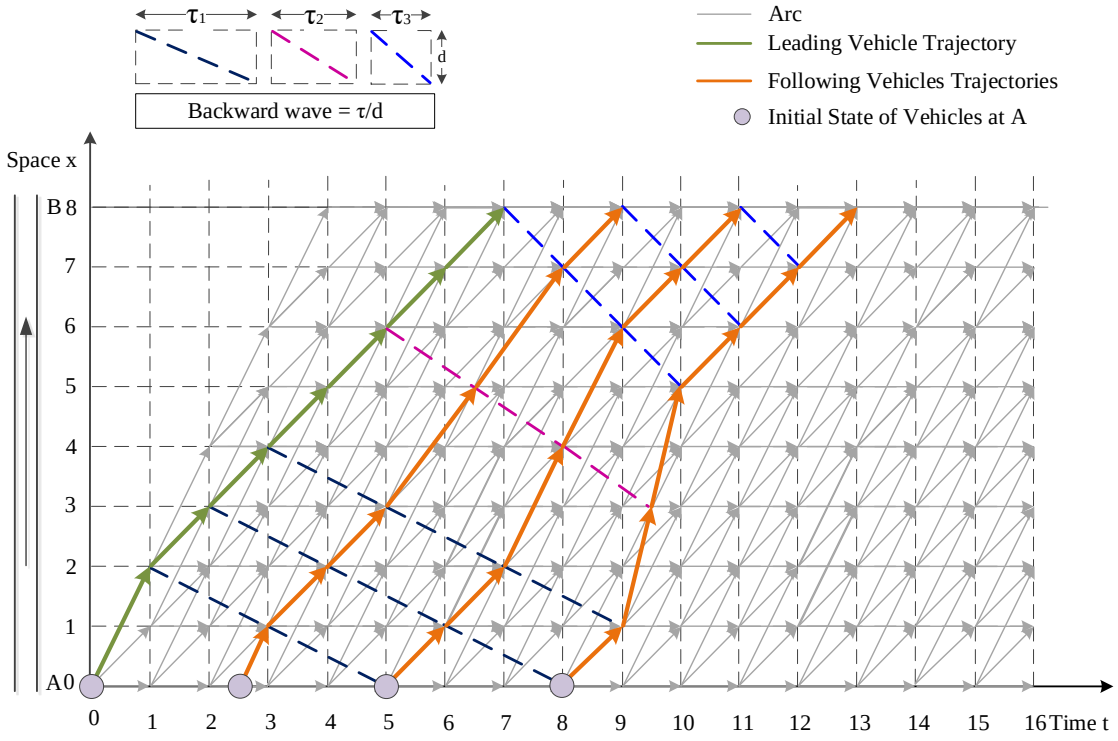


Figure 3.6 Discretized space-time network for vehicle trajectory optimization (1+m(w))

Figure 3.3 shows the possible trajectory of a single optimized autonomous vehicle from point A to point B. This trajectory is used as the leader trajectory for the other trajectory

control modes in Figures 3.4, 3.5 and 3.6. In Figure 3.4 possible trajectories between the lead and the following vehicles are analyzed. The following vehicle starts with free flow speed until it reaches the lead vehicle safety boundary. At that point, the following vehicle adjusts its speed to that of the lead vehicle according to constraint (10). Figure3.5 depicts the trajectories of the optimized leading and multiple following vehicles with fixed reaction time where the leader is controlling the tightly coupled followers. The following vehicles in the platoon travel with the same speed as the leader. However, in the case of the optimized lead AV and multiple tightly coupled following vehicles with variable reaction time, as shown in Figure 3.6, the trajectories of the following vehicles in the platoon vary according to the changing reaction times, according to a given objective function to optimize.

3.3 Formulation and Optimality Conditions in Dynamic Programming for Coupled Vehicles

From the control point of view, it seems to be straightforward to control vehicle' speed and deceleration individually, but it is very complex and challenging to optimize all vehicles' trajectories independently. In our opinion, it is beneficial to first take a platoon-based approach for optimizing and synchronizing the same variable reaction time of m autonomous vehicles, depending on the available vehicle to vehicle communication capabilities, and then accordingly use this group of (optimized) reference trajectories to further apply vehicle speed and acceleration control at an individual level. The dynamic programming proposed for the 4 modes is analyzed in Table 3.2.

Table 3.2 All elements of dynamic programming for all optimization types

No.	**Elements**	**Single vehicle (mode (1))**	**Two vehicles (mode(1+1))**	**Multiple vehicles with fixed displacement time (mode (1 + m))**	**Multiple vehicles with variable displacement time (mode(1+m(w)))**
(1)	Stage	$0,1,..,T$	$0,1,..,T$	$0,1,..,T$	$0,1,..,T$

Table 3.2 (cont'd)

(2)	State	$S = [x_1(t)]$ Location	$S = [x_1(t), x_2(t + \tau)]$ Location of leader, location of follower	$S = [x_1(t)]$ Location of leader, derived locations of followers 2, …, m	$S = [x_1(t), \tau(t)]$ Location of leader, derived locations of followers 2, …, m, reaction time τ for the platoon
(3)	Policy control/ decision variables	$v_1(t), (i.e. x_1(t + 1) - x_1(t)$	$v_1(t), v_2(t + \tau)$	$v_1(t), v_m(t + \tau * m)$	$v_1(t), v_m(t + \tau(t) * m)$, reaction time $\tau(t)$
(4)	Vehicle location updating	$x_1(t + 1) = x_1(t) + v_1(t)$	$x_1(t + 1) = x_1(t) + v_1(t)$ $x_2(t + \tau + 1) = min\{x_2(t + \tau) + v_2(t), x_1(t + 1) - d_2\}$	$x_1(t + 1) = x_1(t) + v_1(t);$ $x_m(t + \tau * m + 1) = min\{x_m(t + \tau * m) + v_m(t), x_1(t + 1) - d_m * m\}$	$x_1(t + 1) = x_1(t) + v_1(t);$ $x_m(t + \tau(t) * m + 1) = min\{x_m(t + \tau(t) * m) + v_m(t), x_1(t + 1) - d_m * m\}$
(5)	Cost function for both control and derived variables:	$c[x_1(t), x_1(t + 1)]$	$c[x_1(t), x_1(t + 1), x_2(t + \tau), x_2(t + \tau + 1)]$	Cumulative cost across all vehicles in a platoon $cc[x_1(t), x_1(t + 1), x_2(t + \tau), x_2(t + \tau + 1, \dots, x_m(t + \tau * m), x_m(t + 1 + \tau * m)]$	Cumulative cost across all vehicles in a platoon $cc[x_1(t), x_1(t + 1), x_2(t + \tau(t)), x_2(t + \tau(t) + 1, \dots, x_m(t + \tau(t) * m), x_m(t + 1 + \tau(t) * m)$

Table 3.2 (cont'd)

(6)	Value function for control variables	$L(t, x_1(t))$	$L(t, x_1(t), x_2(t + \tau))$	$L(t, x_1(t))$	$L(t, x_1(t), \tau(t))$

(1) Stage: based on the discretized time in the space-time network for mode (1), mode (1+1), mode (1+m) and in space-time-reaction time network for mode (1+m(w)), all modes can have the same stage from time 0 to time T;

(2) State: For mode (1), its state can be represented by location only as $S = [x_1(t)]$. For example, if the space-time network in Figure 3.3 is built for mode (1), the possible states are {0, 1, 2} when time is 1 depends on selected velocity.

For mode (1+1), since the two vehicles need to keep a safety spacing, we can represent the state as a safe-driving state vector with two dimensions as $S = [x_1(t), x_2(t + \tau)]$. If the space-time network in Figure 3.4 is used for illustrating mode (1+1), in order to satisfy constraint (10), the safety states are {0, 1, 2, 3, 4} at time 6.

Mode (1+m) considers the lead vehicle position as the state and then derives the locations for multiple following vehicles by using constant reaction time. Thus, we only have one independent state represented as an one-dimensional vector $S = [x_1(t)]$, shown in Figure 3.3.

Mode (1+m(w)) adds variable reaction time into the state vector of mode (1+m), so the state in the platoon is represented as $S = [x_1(t), \tau(t)]$, shown in Figure 3.6.

(3) Control: For mode (1), the control/ decision variable is the speed of optimized vehicle $v_1(t)$. There are two control/ decision variables in mode (1+1): the speed of the lead vehicle at time t, $v_1(t)$, and the speed of the following vehicle at a different time index $t + \tau, v_2(t + \tau)$. For mode (1+m), the control/ decision variable for the leading vehicle is $v_1(t)$. Mode (1+m(w)) considers two control variables $v_1(t)$ and $\tau(t)$, which further determine the remaining following vehicles' trajectories (as derived variables).

(4) Cost function of decisions used in optimality conditions: Mode (1) and mode (1+1) can be represented as $c[x_1(t), x_1(t + 1)]$ and $c[x_1(t), x_1(t + 1), x_2(t + \tau), x_2(t + \tau + 1)]$, respectively. The total system travel cost for multiple vehicles can be calculated by summing each vehicle's cost cumulatively in the platoon. The cumulative cost value in

the case of platoon trajectory control for mode (1+m) and for mode (1+m(w)) can be represented as $cc[x_1(t), x_1(t+1), x_2(t+\tau), x_2(t+\tau+1), \dots, x_m(t+\tau*m), x_m(t+1+\tau*m)]$ and $cc[x_1(t), x_1(t+1), x_2(t+\tau(t)), x_2(t+\tau(t)+1), \dots, x_m(t+\tau(t)*m), x_m(t+1+\tau(t)*m)$, respectively.

If the capacity consumption is concerned for a tight car-following platoon, we can consider as maximum completion time as the cost of platoon, shown as the along time 0 to $(t+m*\tau)$ in Figure 3.7. Please note that, the reaction time τ is a variable in this mode, thus the selection of τ would affect the boundary of the platoon. That is, a smaller reaction time can reduce the platoon footprint in the space-time diagram.

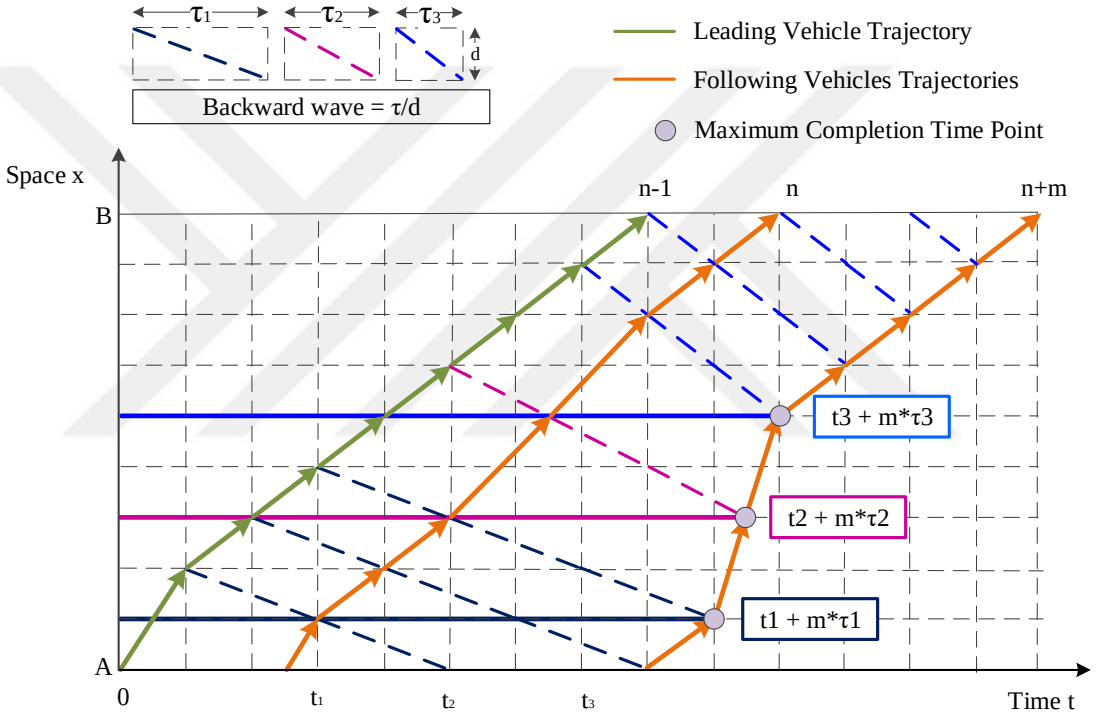


Figure 3.7 Illustration of maximum completion time

(5) Value function: This is described as the cumulative value from stage 0 to the current stage. For both mode (1) and mode (1+m), it can be represented as $L(t, x_1(t))$. Since the two vehicles are controlling in mode(1+1), the label cost can be represented as $L(t, x_1(t), x_2(t+\tau))$as a 3-dimenstional vector. mode (1+m(w) also a 3-dimenstional label cost vector as $L(t, x_1(t), \tau(t))$, because of controlling multiple vehicle trajectories and reaction time.

The aforementioned problem contains two principle features: (1) it is in essence a discrete-time (e.g., every second) dynamic (i.e., time-dependent) system; (2) the total cost is additive in a sense that the generalized cost incurred at time k is accumulated over time.

The system's state at time $t+1$ is only determined by the decisions made at t and its previous state at t. As a result, the optimal vehicle trajectories can be solved by using dynamic programming. Those algorithms mentioned in Table 3.2 will be stated in detail in section 3.3.

3.4 Dynamic programming algorithms

3.4.1 Mode ("1")

The DP-based optimization algorithm for mode (1) is described as below:

We denote D as the total distance under consideration, d^{max} as the maximum distance one vehicle can travel at one time step, $L(t, x(t))$ as the value function of state $x(t)$ at t, $t \in [0, T], x \in [0, D]$, d^{max} as the maximum distance one vehicle can travel at one time step (equal to v_{max} in this research), and the initial $L(t, x(t))$ values are all positive infinity.

```
// initialization
L(t, x_1(t)) := +∞;  // value of state (x_1(t))
L(0, x_1(0)) := 0;
for t = 0 to T do
    for x_1(t) = 0 to D  (within the feasible range) do
        for x_1(t+1) = x_1(t) to min{D, x_1(t) + d^max} do
            if x_1(t) and x_1(t+1) are within feasible space-time regions;
               and  L(t, x_1(t)) + c[x_1(t), x_1(t+1)] < L(t+1, x_1(t+1))
            then L(t+1, x_1(t+1)) = L(t, x_1(t)) + c[x_1(t), x_1(t+1)];
        endfor;
    endfor;
endfor;
```

After all iterations, search the corresponding time index with the minimal label cost at D and trace back to get the optimal vehicle trajectory. Total cost$(t = T^*, x = D) =$

$\min_t\{\mathrm{L}(\mathrm{t},\mathrm{x}=\mathrm{D})\}$, where T^* is the time index leading to the minimum cost value at distance D.

3.4.2 Mode ("1+1")

Denote $L(t, x_1(t), x_2(t+\tau))$ as the value function of state$(x_1(t), x_2(t+\tau))$ at t, $t \in [0, T], x \in [0, D]$.

01 // initialization

02 $L(t, x_1(t), x_2(t+\tau)) := +\infty$; // value of state $(x_1(t), x_2(t+\tau))$

03 $L(t, x_1(0), x_2(0+\tau)) := 0$;

04 **for** $t = 0$ to T **do**

05 **for** $x_1(t) = 0$ to D **do**

06 **for** $x_2(t+\tau) = 0$ to $x_1(t) - d$ **do**

07 **for** $x_1(t+1) = x_1(t)$ to $x_1(t) + d^{max}$ **do**

08 **for** $x_2(t+\tau+1) = x_2(t+\tau)$ to $\min\{x_1(t+1) - d, x_2(t+\tau) + d^{max}\}$ **do**

09 **if** $x_1(t), x_1(t+1), x_2(t+\tau), x_2(t+\tau+1)$ are within feasible space-time regions;

and $L(t, x_1(t), x_2(t+\tau)) + c(x_1(t), x_1(t+1), x_2(t+\tau), x_2(t+\tau+1)) < L(t+1, x_1(t+1), x_2(t+\tau+1))$

10 **then** $L(t+1, x_1(t+1), x_2(t+\tau+1)) = L(t, x_1(t), x_2(t+\tau)) + c(x_1(t), x_1(t+1), x_2(t+\tau), x_2(t+\tau+1))$;

11 **endfor;**

12 **endfor;**

13 **endfor;**

14 **endfor;**

15 **endfor;**

Because the final arrival times at the space boundary are not fixed, we need to search the corresponding time indices of two vehicles with the minimal label cost at *D* and trace back to obtain the optimal vehicle trajectory of each vehicle respectively.

3.4.3 Mode ("1+m")

Denote $L(t, x_1(t))$ as the value function of state$(t, x_1(t),\ldots, x_m(t+\tau*m))$ at t, $t \in [0, T], x \in [0, D]$ and cc as the cumulative cost function from vehicle 1 to vehicle m in the platoon.

01 // initialization

02 $L(t, x_1(t)) := +\infty$;

03 $L(t, x_1(0)) := 0$;

04 **for** $t = 0$ to T **do** **//stage**

05 **for** $x_1(t) = 0$ to D **do //state**

06 **for** $x_1(t+1) = x_1(t)$ to $x(t) + d^{max}$ **do** //control decision

07 $cc = c[x_1(t), x_1(t+1)]$

08 **for** $m = 1$ to M **do**

09 $x_m(t+\tau*m+1) = \min\{(x_m(t=0) + v_f \times (t + \tau*m+1), x_1(t) - \sum_{i=2}^{m} d_i\}$ //(vehicle m's position

10 $cc = cc + c[x_m(t+\tau*m), x_m(t+\tau*m+1)]$; // cost of decision

11 **endfor;**

12 **if** $x_1(t)$, $x_1(t+1)$, $x_2(t+\tau)$, $x_2(t+\tau+1)$, …, $x_m(t+\tau*m), x_m(t+\tau*m+1)$ are within feasible space-time regions **and** $L\big(t, x_1(t)\big) + cc < L(t+1, x_1(t+1))$

13 **then** $L(t+1, x_1(t+1)) = L(t, x_1(t)) + cc$;

14 **endfor;**

15 **endfor;**

16 **endfor;**

3.4.4 Mode ("1+m(w)")

Denote $L(t, x_1(t), \tau(t))$ as the value function of state $S = [x_1(t), x_m(t + \tau(t) * m)]$ at t, $t \in [0, T], x \in [0, D], \tau \in [0, \tau]$ and cc as the cumulative cost function from vehicle 1 to vehicle m in the platoon. Assume $\tau_U(d)$ as the maximum reaction time along d to D, $\tau_L(d)$ as the minimum reaction time supported by a selected communication technology along d to D, $\tau_{change}(t)$ as a binary variable along t to T satisfying the reaction time changing constraints in Eqs. (12), (13) and (14). By using the extended Newell's inequality constraint for multiple vehicles in Eq. 11 and control decision for leading vehicle as written $x_1(t+1) = x_1(t)$ to $x_1(t) + d^{max}$, the flow balance constraint is always ensured by controlling whether or not any vehicle visits 3D vertex (i, t, τ). In this proposed multi-vehicle control model, we can solve the semi-open boundary optimization problem, by only defining the initial position of vehicles, by building a time-space-reaction time network with the desired objective, such as emissions, fuel consumption, travel time etc.

The DP-based optimization algorithm is described as below:

01 // initialization

02 $L(t, x_1(t), \tau)) := +\infty$; // value of state $(x_1(t))$

03 $L(t = 0, x_1(0), \tau)) := 0$;

04 **for** $t = 0$ to T **do** // 1st loop: time stage

05 **for** $x_1(t) = 0$ to D **do** //2nd loop: feasible space state

06 **for** $x_1(t+1) = x_1(t)$ to $x_1(t) + d^{max}$ **do** //3rd loop: speed control decision

07 **for** $\tau = \tau_L(x_1(t))$ *to* $\tau_U(x_1(t))$ **do** //4th loop: reaction time levels

08 **for** $\tau' = \max(\tau - \tau_{change}, \tau_L(x_1(t)))$ *to* $\min(\tau + \tau_{change}, \tau_U(x_1(t)))$ **do** // 5th loop: reaction time change

09 $cc = c[x_1(t), x_1(t+1)]$

10 **for** $m = 1$ to M **do** //6th loop: number of vehicles in a platoon

11 $x_m(t+\tau' * m+1) = \min\{(x_m(t=0) + v_f \times (t+\ \tau' * m+1), x_1(t) - \sum_{i=2}^{m} d_i\}$ // vehicle m's position

12 $cc = cc + c[x_m(t+\tau * m), x_m(t+\tau' * m+1)]$;// cost of decision

13 **endfor;**

14 **if** $x_1(t)$, $x_1(t+1)$, $x_2(t+\tau)$, $x_2(t+\tau+1)$, …, $x_m(t+\tau * m), x_m(t+\tau * m+1)$ are within feasible space-time regions; and $L\big(t,\tau,x_1(t)\big) + cc < L(t+1, x_1(t+1), \tau')$

15 **then** $L(t+1, x_1(t+1), \tau') = L(t, x_1(t), \tau) + cc$

16 **endfor;**

17 **endfor;**

18 **endfor;**

19 **endfor;**

20 **endfor;**

As stated in chapter 20 in the book by Jensen and Bard, the dynamic programming approach has two different types of recursion relationships: backward recursion and forward recursion [77]. As shown in our platoon trajectory optimization problem Mode "1+m", we use the following label cost updating functions (3.6) to implement the forward recursive equation (27):

If $L\big(t, x_1(t)\big) + cc < L(t+1, x_1(t+1))$ **then** $L(t+1, x_1(t+1)) = L(t, x_1(t)) + cc$; (3.6)

Forward recursive equation

$L(t+1, x_1(t+1)) = Min\ \{L\big(t, x_1(t)\big) + cc\}$ for time stage t=0, 1, …, T (3.7)

where cc is the cumulative cost across all vehicles in the platoon at time t ; and the vehicle location states are subject to the following two constraints.

$x_1(t+1) = x_1(t) + v_1(t)$;

$x_m(t+\tau * m+1) = min\ \{x_m(t+\tau * m) + v_m(t), x_1(t+1) - d_m * m\}$

One can use a backward recovery procedure to identify the optimal path from the final state associated with the minimum label cost. A detailed discussion on the equivalent relationship between backward induction and forward induction can be also found in chapter 11 of the book by Bradley, Hax, and Magnanti [78]. In short, the procedure in our paper uses a forward recursive function from one-time stage to a successor time stage, so the overall solution searching framework still follows a dynamic programming approach.

On the other hand, one could re-express the proposed forward DP model using a backward recursive search relationship and we do believe this backward approach is much closer to the original open-loop feedback control framework in standard DP. However, the classical backward (closed-loop) approach requires (i) a clear definition of the ending states and associated boundary conditions at time T and (ii) the initial state at time t=0 can be backward reachable from the defined ending states. In comparison, our proposed forward approach is more suitable for propagating the current initial states of the platoon into the (partially unknown) future states and one can select one of feasible ending states as the final optimal solution to back trace to the initial boundary.

It should be further remarked that, the model of 1+m(w) treats reaction time as discrete variables, so our problem indeed changes the feasible space compared with the original problem of controlling all vehicles with continuous reaction times. Under this feasible space, we only keep the best feasible solutions at each space-time-state vertex with the minimal label cost, and the other dominated solutions are pruned by the optimality conditions. If an enumeration algorithm is used (instead of our proposed DP algorithms), then one has to explore all possible paths from the beginning which might still contain many sub-optimal sub paths based on our proposed optimality criteria.

3.5 Time complexity of algorithms

We need to specify the time complexity of the proposed DP algorithms especially mode "1+m(w)" because of having multiple loops. We can annotate the maximum iteration counts in the algorithm as for the first two loops with the time and space indexes, T_N and D_N, the 3rd loop for displacement in the grid, d_N, the 4th loop for number of reaction time levels, τ_N, the 5th loop for number of reaction time levels, $\Delta\tau_N$, and finally the 6th loop for vehicles count in platoon, M_N. Because of having only linear increasing iterations in the loops of the algorithm we can conclude the time complexity of mode "1+m(w)" in big O notation form as O($T_N\, D_N d_N \tau_N \Delta\tau_N M_N$).

3.6 Improving computational complexity

As there are multiple loops in the proposed DP algorithm, we need to carefully examine its efficiency on a discretized network. For the first two loops with the time and space indexes, one can greatly reduce the space search range by considering the feasible prism of the vehicle trajectories, and a time geography based approach has been systematically discussed by Zhou et al. [79].

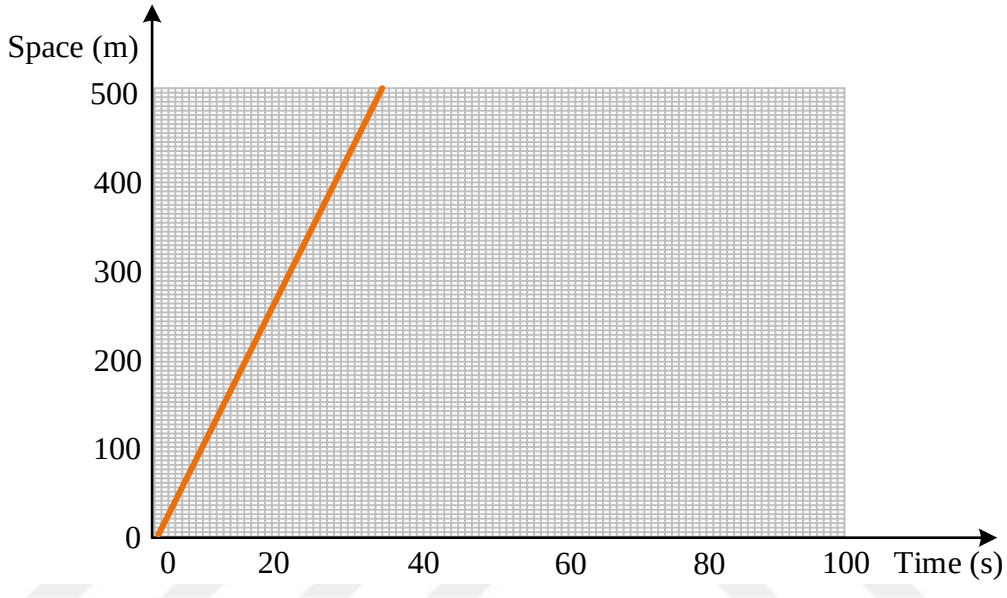


Figure 3.8 Illustration of full search space for mode 1+m(w)

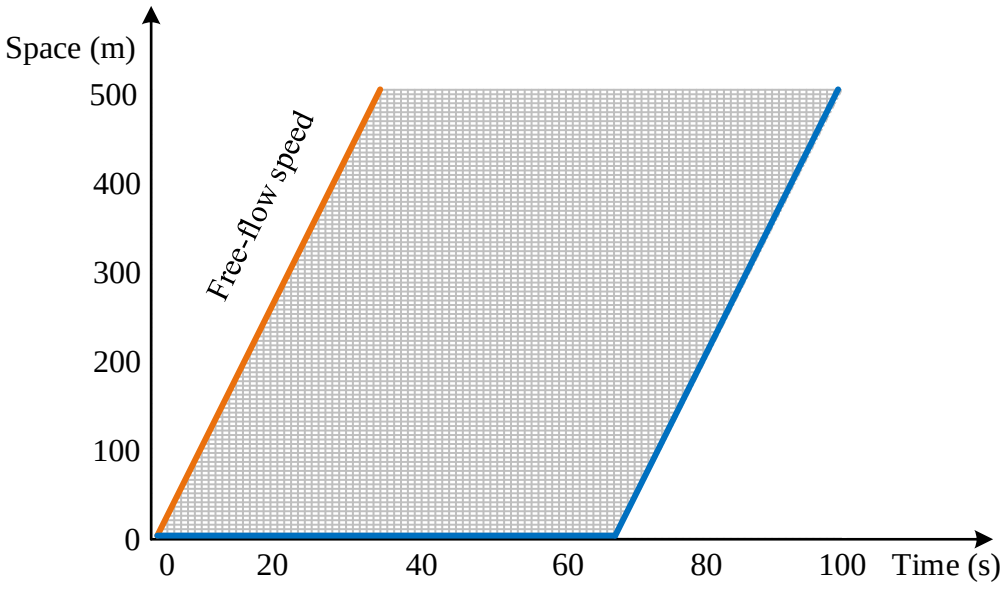


Figure 3.9 Illustration of reduced search space for mode 1+m(w)

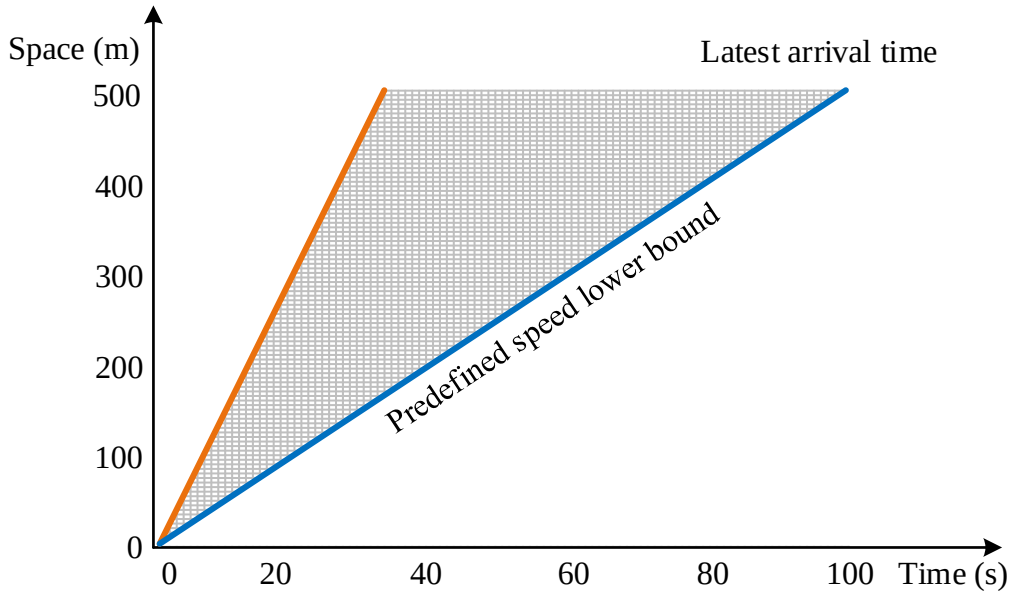


Figure 3.10 Illustration of reduced search space with optimized step size for mode 1+m(w)

The 3rd loop is related to the maximum number of steps considered in the discretized grid, e.g., around 8-20 steps used in our experiment. The 4th loop is related to the number of reaction time levels, e.g., 4 levels for a maximum reaction time of 2 s. The 5th loop requires very limited efforts, as typically only very smooth changes (e.g., 0, 1, 2 steps) in reaction times are allowed. The last loop considers all the vehicles in a platoon, typically in a size of 2-4. Overall, even there are multiple nested loops in the proposed DP algorithm, many loops as associated with very small values and we could further intelligently reduce the search efforts by selecting the most likely and most promising state changes in order to avoid the curse of dimensionality.

Reducing search space in the discretized network is a potentially useful approach to improve the computational efficiency. For this purpose, we perform experiments to demonstrate how to reduce search space by selecting feasible space-time grid cells and maximum number of steps values for 2nd and 3rd loops. Figures 3.8, 3.9 and 3.10 show three different search spaces: full search space without any optimization (Figure 3.6), reduced search space by assuming maximum speed limit and preferred latest arrival time as the space boundary (Fig 3.9), and reduced search space with optimized step size by additionally selecting desirable speed lower bound (Figure 3.10). Table 3.3 shows the resulting CPU running time by using a kind of traditional personal computer which has i7 CPU 2.4 GHz, 8 GB RAM, 256 GB SSD and optimizing steps for (Figure 3.9) and (Figure 3.10) in bold, for applying search space reduction before as (Figure 3.8) and after

as (Figure 3.9) and (Figure 3.10), as 17.55 s, 13.24 s and 9.72 s, leading to an about 55% reduction in CPU time due to reduced search space.

Table 3.3 Processing time for three different cases

	a)	b)	c)
Time and space by using 0.5 s and 0.5 meters as simulation resolution, 1st and 2nd loops	$200*10^3$	$134*10^3$	$134*10^3$
Maximum number of the steps, 3rd loop	16	16	8
Reaction time levels, 4th loop	4	4	4
$\Delta\tau$, 5th loop	1	1	1
Vehicle count, 6th loop	5	5	5
Total	$6400*10^4$	$4288*10^4$	$2144*10^4$
CPU running time (s)	17.55	13.94	9.72

In addition, the possibility of considering the proposed trajectory control in a more complex condition, such as, the process of merging, is discussed in Appendix A.

CHAPTER 4

NUMERICAL EXPERIMENTS

In this section, we perform experiments to demonstrate how to optimize vehicle trajectories by using dynamic programming. DP algorithms are performed for "1"(optimizing trajectory of one automated vehicle and comparing the emission with typical vehicle), "1+1" "(optimizing trajectory of two automated vehicles and comparing the emissions with typical vehicles), "1+m"(one lead automated vehicle control with considering the impacts to m human-driven following vehicles, which could be further organized as a platoon) and "1+m(w)" (one leading automated vehicle and m following automated vehicle's reaction time control.

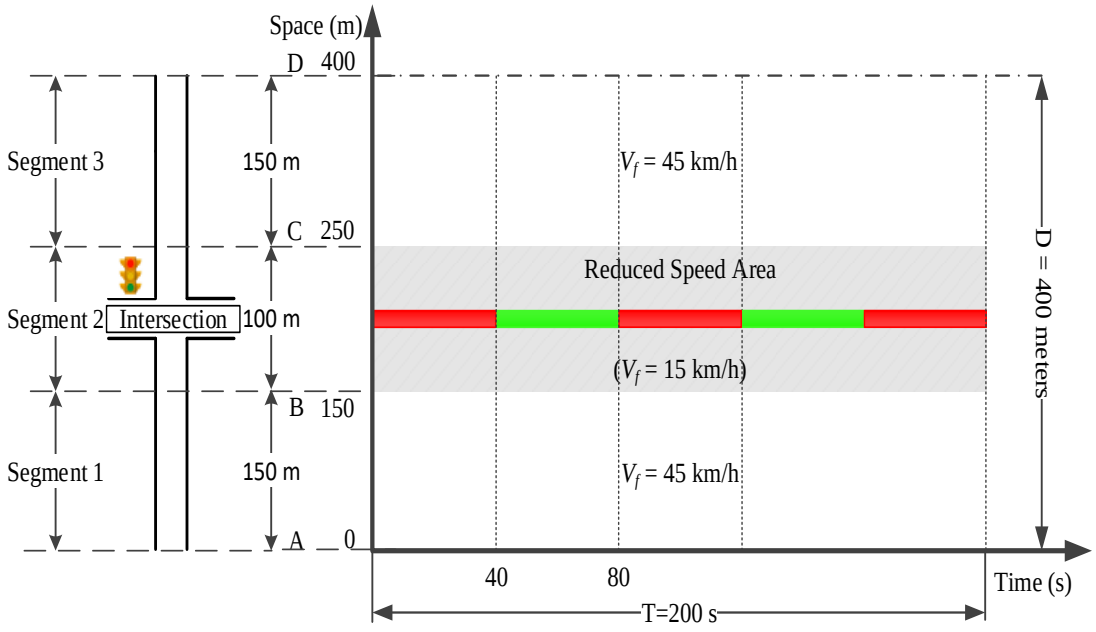


Figure 4.1 Hypothetical environment for the experiments for Modes "1" and "1+1"

Figure 4.1 shows the hypothetical environment for the experiments for Modes "1" and "1+1". The total length of the road segment is 400 meters and maximum time horizon is

200 seconds; the speed limit is 45 kilometers per hour and from 150 meters to 250 meters is the speed-reduction zone with the speed of 15 kilometers. At 200 meters is a traffic signal where the red phase duration is 30 s and green is 50 s. For the configuration of Newell's car-following model, we set$\tau = 2s$, $d0 = 2m$. Vehicle emissions are calculated based on vehicles' instantaneous speeds. Vehicle emissions are calculated based on vehicles' instantaneous speeds [80].

4.1 Trajectory Analysis of one AV by Using Mode "1"

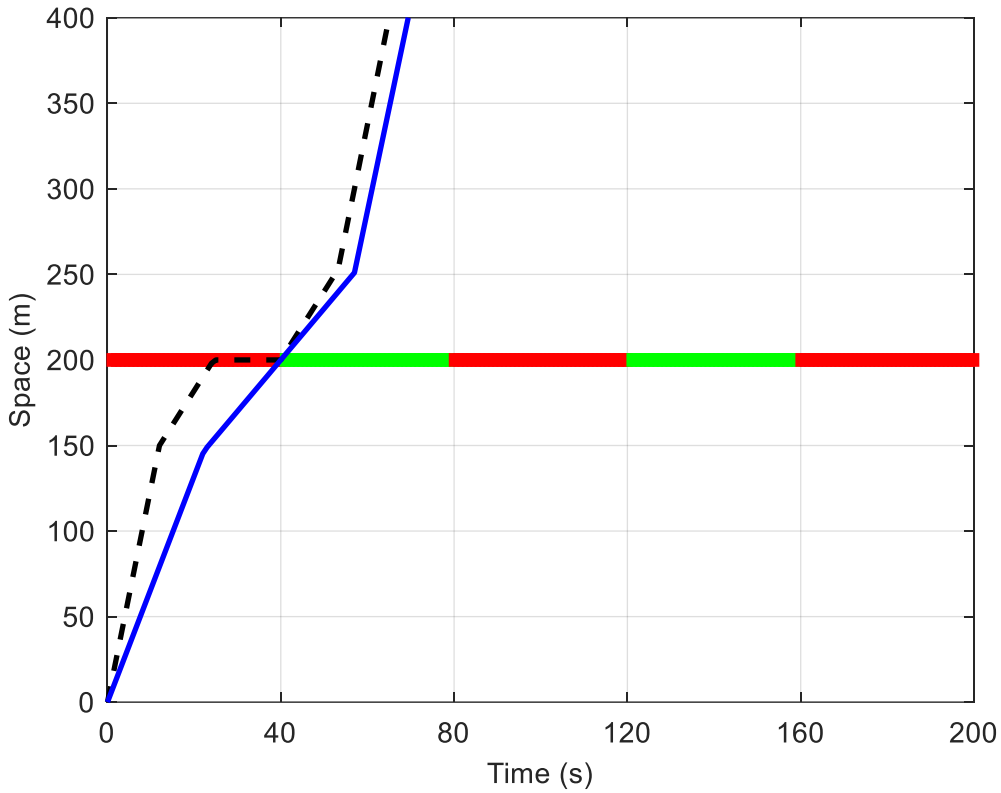


Figure 4.2 Optimal trajectory for Mode "1"

In this experiment, we optimize one vehicle's trajectory from zero to D so to minimize its travel time. Assuming vehicle's initial speed is 0, vehicle trajectories are optimized using dynamic programming over time. Figure 4.2 shows the optimal vehicle trajectory and speed incurring the minimal travel time and the typical trajectory and speed under the same condition. The resulting emissions under the best fuel efficiency trajectory for minimal travel time for AV (solid blue line) and typical vehicle (dashed black line) (based on [81]) is 0.78 gram and 1.02 gram respectively, a 23.81% emission reduction. However, the travel time of AV will be longer than typical vehicle.

4.2 Trajectory Analysis of two simultaneous AVs by Using Mode “1+1”

In this experiment, we consider two vehicles within the scope and their trajectories are optimized simultaneously. The finding of this experiment is particularly useful in automated vehicle research because this experiment can be easily extended to identify when two fleets should merge into one bigger fleet and when these two fleets should be split into smaller fleets while many automated vehicles are on the road. Following the DP algorithm Mode”1+1” described in Section 3.3.2, Figure 4.3 shows the optimal trajectories of two vehicles. From Figure 4.3, we can tell that both vehicles prefer to drive in a way to avoid stops at intersections. Figure 4.3 compares the optimal trajectories for two AV and typical trajectories of two typical vehicles. In this experiment, the resulting emission of two AVs from optimal trajectories (leader: solid blue line and follower: solid brown line) and emission of two vehicles from typical trajectories (first vehicle: dashed black line and second vehicle: dashed-dotted black line) are 1.69 gram and 2.13 gram respectively, a 21.7% reduction in fuel consumption.

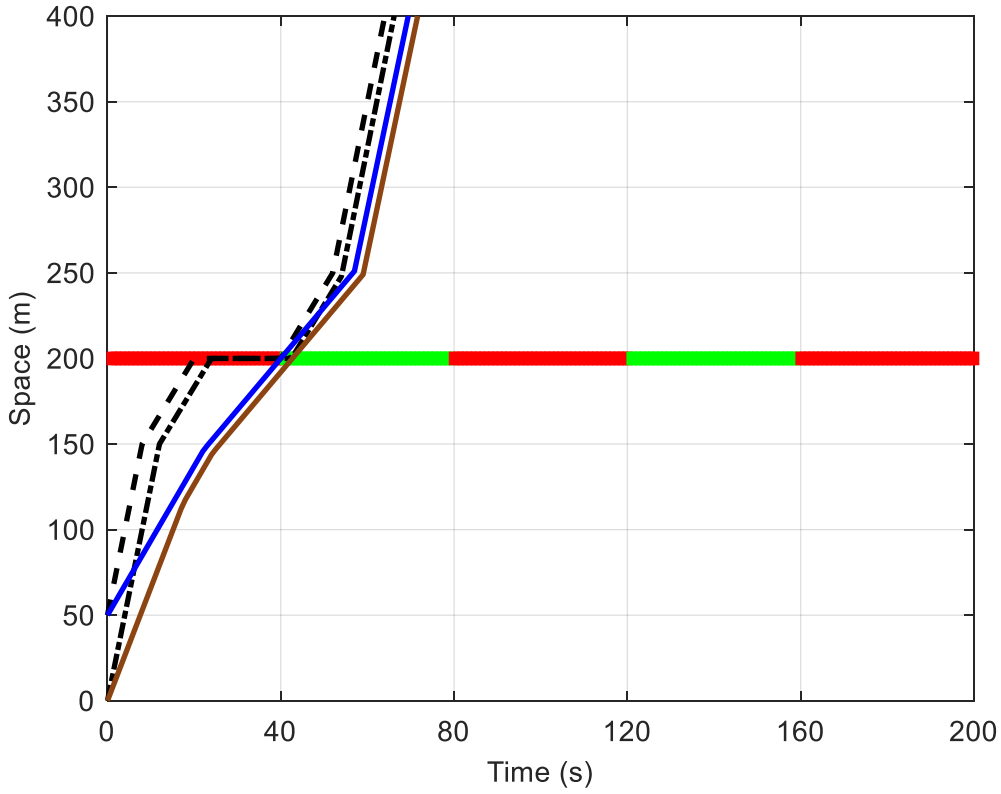


Figure 4.3 Optimal trajectories for Mode “1+1”

4.3 Platoon Analysis by Using Mode "1 + M" for Automated Vehicles with Surrounding Obstacles

One challenge of deploying autonomous vehicles in the real world is to consider the influence from moving obstacles (e.g. human-driving vehicle) and static obstacles (e.g. stuffs left unintentionally on roads). In this section, we perform experiments to demonstrate how to optimize vehicle trajectories for avoiding moving obstacles, which can be detected in real time by sensors from autonomous vehicles. Since the mode is still at "1+m", the lead autonomous vehicle is just under control and its following autonomous vehicles have a fixed reaction time and adjust their trajectory based on the change of the lead vehicle.

Hypothetical layout of experiments has been illustrated in Figure 4.4, human operated vehicles trajectories have been shown in Figure 4.5 and Figure 4.6. Further experiments only for lane 2, human operated vehicles which identification numbers are 3360 and 488 have been excluded in Figure 4.6. AVs and human operated vehicles trajectories from origin to destination and zooming view of highlighted region have been shown Figure. 4.7 and Figure. 4.8, respectively. Zooming view of AVs and human operated vehicles trajectories have been shown in Figure 4.9 and Figure 4.10 which highlighted in Figure 4.7 and Figure 4.8, respectively. Table 4.1 shows the maximum MSR values in mixed traffic condition for lane 1. As can be seen, MSR increases as reaction times decrease. Also for lane 2, in heavy traffic condition, MSR increases 50% by excluding only two human operated vehicles.

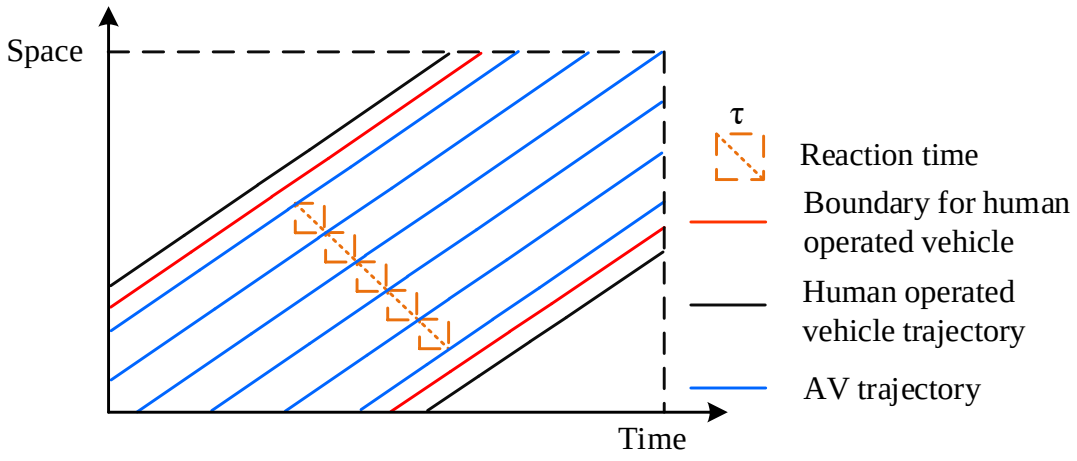


Figure 4.4 Hypothetical layout of experiments

Figures 4.5, 4.6, 4.7, 4.8, 4.9 and 4.10 show AV's trajectories by using mode (1+m) with surrounding real-world human driving car trajectories obtained from the NGSIM project

for I-80 in California [81]. Trajectories of human operated vehicles on lane 1 and lane 2 have been used for experiments where identification numbers are 1247, 1253, 1255, 1284, 1297, 1306 and 1325; 3360, 417, 436, 447, 448, 459, 469, 472, 488, 494 and 507 respectively. The total length of the road segment is 500 meters and the speed limit is 70 miles per hour. For the configuration of Newell's car-following model, we set $d_0 = 2m$ and τ is fixed as 0.5 to show mixed traffic condition trajectories.

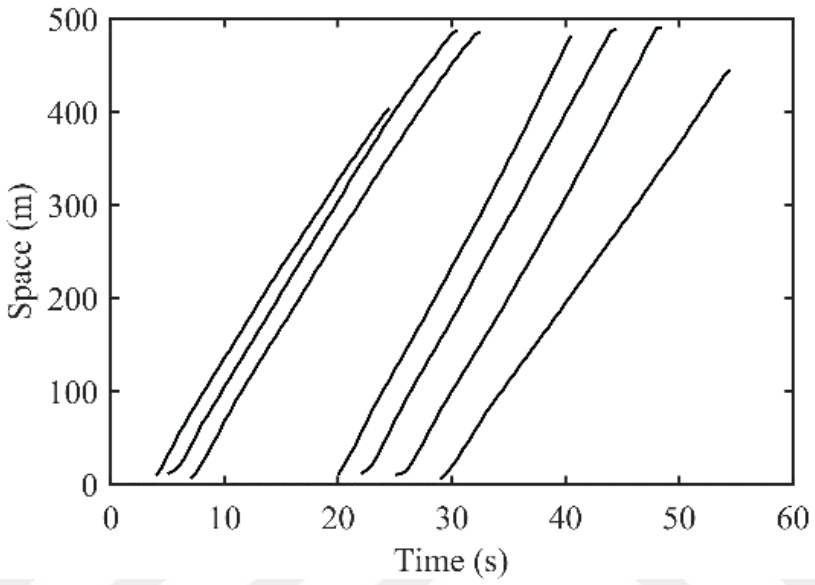


Figure 4.5 Human-operated vehicle trajectories for NGSIM data 101 lane 1

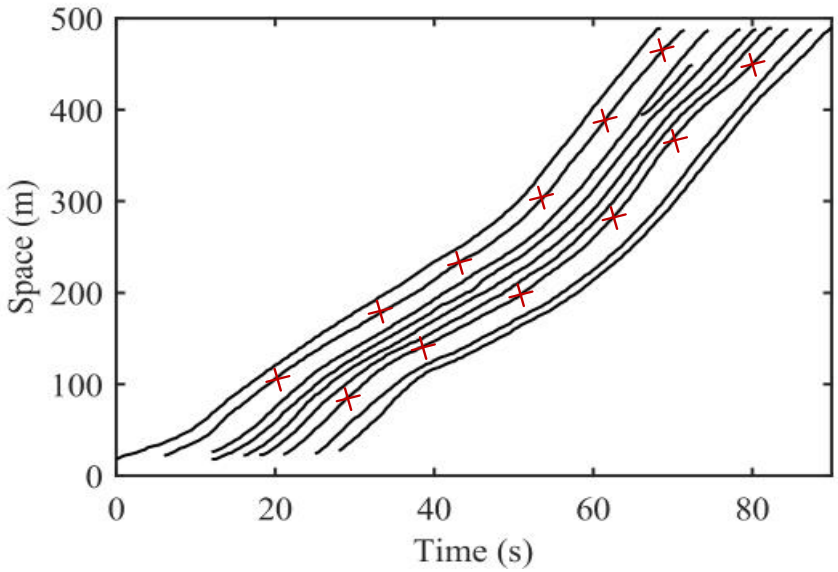


Figure 4.6 Human-operated vehicle trajectories for NGSIM data 101 lane 2

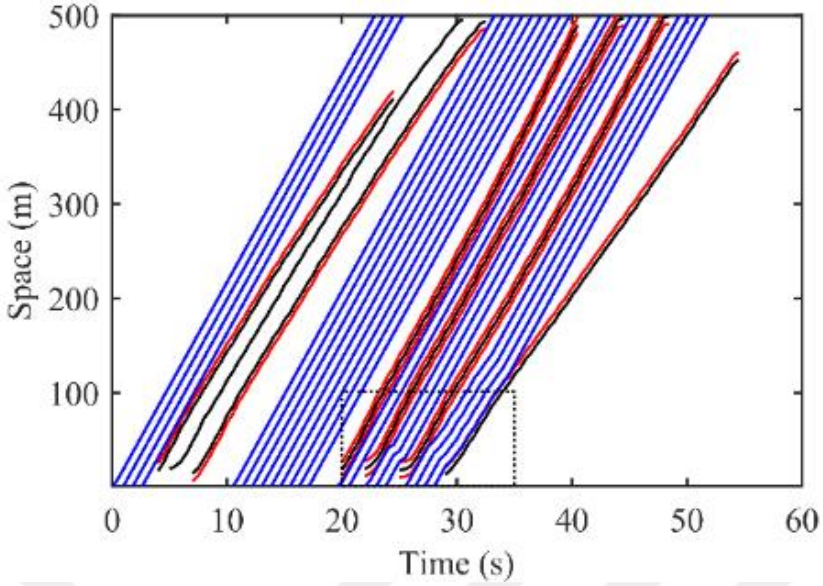


Figure 4.7 Mixed traffic conditions when reaction time equals 0.5 s for lane 1

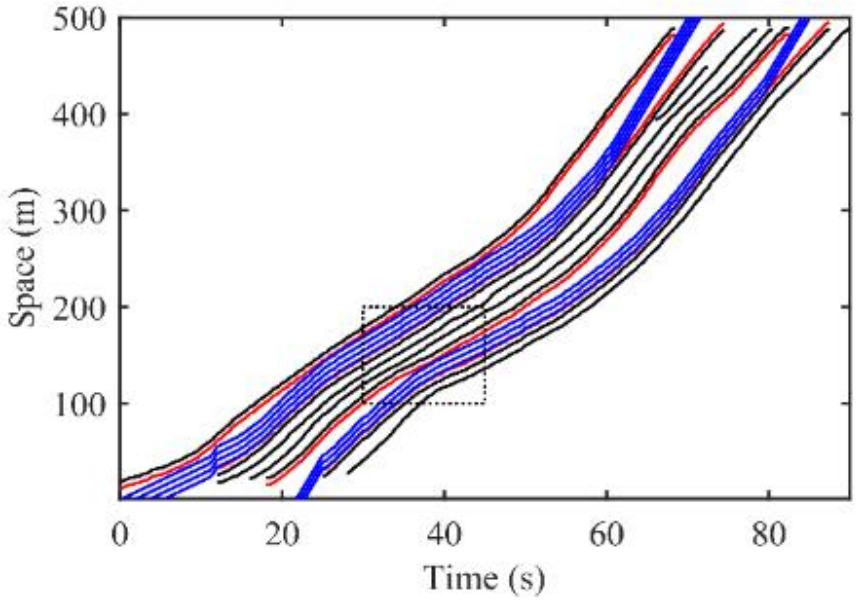


Figure 4.8 Mixed traffic conditions when reaction time equals 0.5 s for lane 2

Table 4.1 MSR (vphpl) by using different reaction times with moving obstacles.

Human-operated vehicles	Human-operated and AVs with different reaction time (s)			
	$\tau = 1.5$ s	$\tau = 1$ s	$\tau = 0.5$ s	$\tau = 0$ s
458	1047	1309	1898	3665

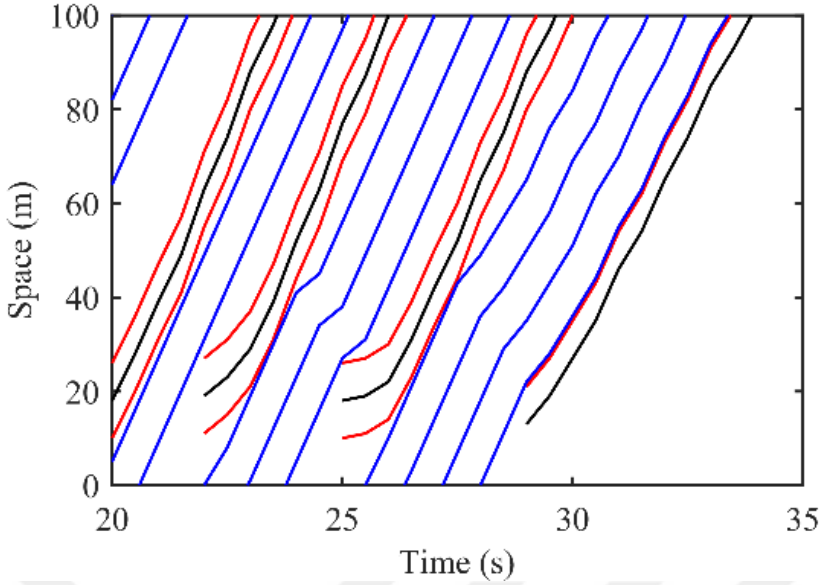


Figure 4.9 Zooming view of mixed traffic conditions which highlighted in Figure 4.7 for lane 1

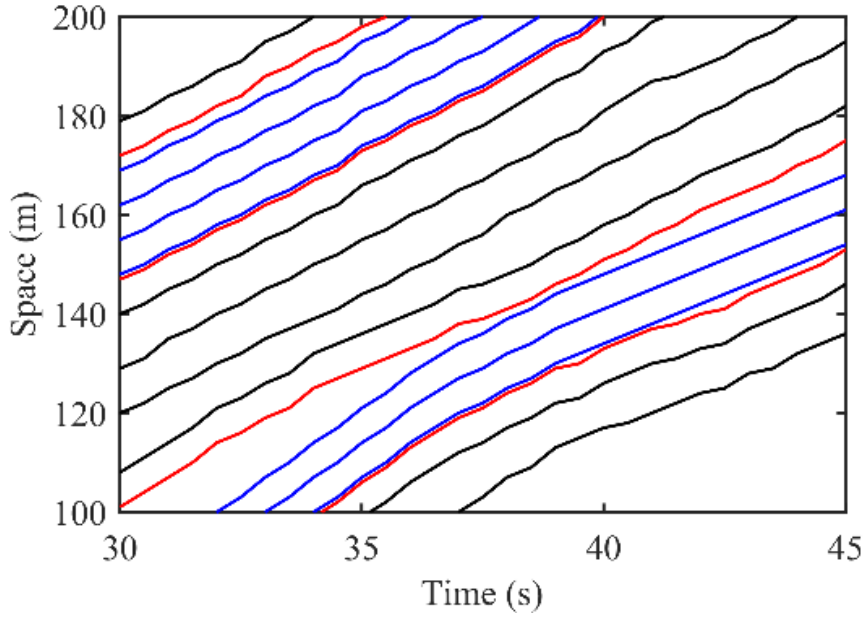


Figure 4.10 Zooming view of mixed traffic conditions which highlighted in Figure 4.8 for lane 2

4.4 Platoon Analysis by using Mode "1 + m (w)"

Figure 4.11 shows the layout of hypothetical environment, where the total length of the road segment is 1000 m and total time horizon is 150 s; the free flow speed is 60 kilometers per hour in segment 1 and segment 3, from origin to 250 meters and from 750 meters to 1000 meters, respectively. Segment 2 is a speed-reduction zone with the speed of 30 km/h from 250 meters to 750 meters. At 250 meters is a traffic signal where the red

phase duration is 20 s and green is 15 s. In addition, there is a traffic signal at 750 meters where the red phase duration is 35 s and green is 20 s.

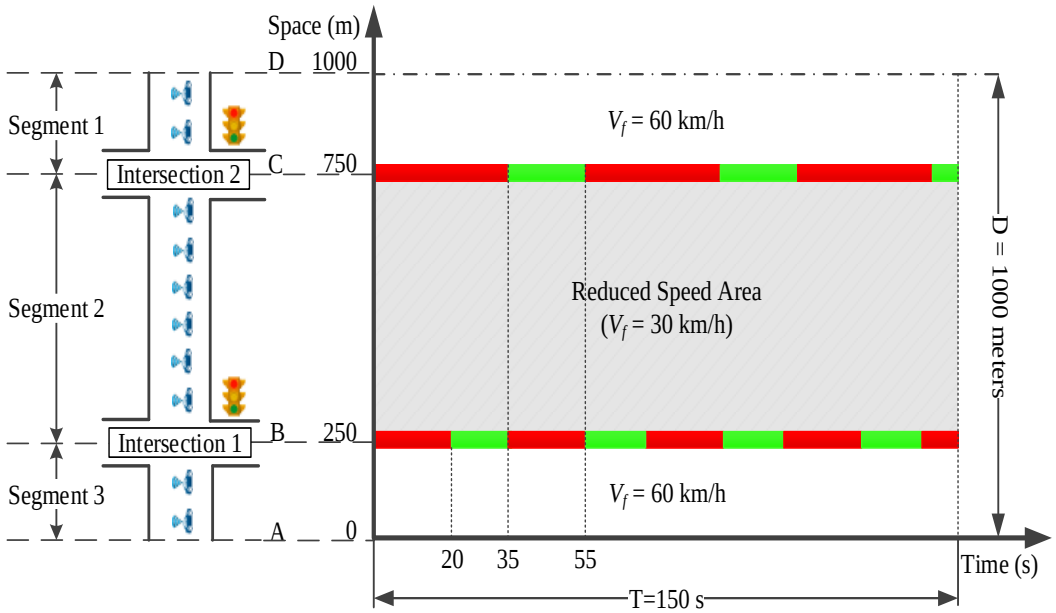


Figure 4.11: Layout of hypothetical road segment

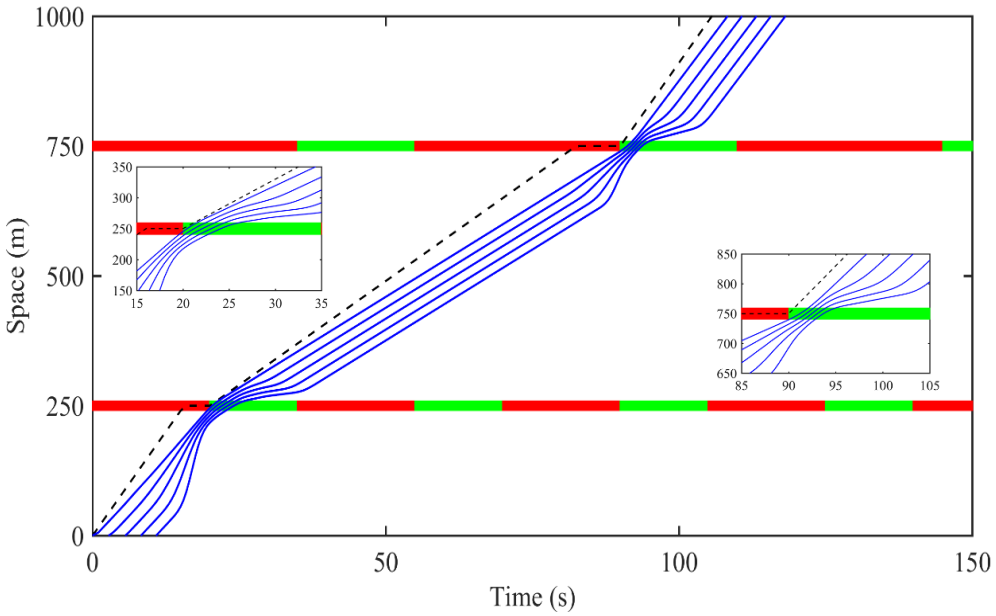


Figure 4.12: Optimal vehicle trajectories by using mode '1+m(w)' without speed limit in transition process

The trajectory of the leader vehicle and reaction time in a platoon have been optimized to obtain the minimum total system travel time after reaching its destination. For the configuration of Newell's car-following model, we set the rear-to-end distance $d_0 = 2\ m$

and τ is variable at intersection regions between 2 s to 0 s with the step size of reaction time change is 0.2 s. There are 5 tightly coupled autonomous and connected vehicles along a one-lane roadway. Figure 4.12 and Figure 4.13 show a typical vehicle trajectory as a black dash line and optimal AVs trajectories as solid blue lines.

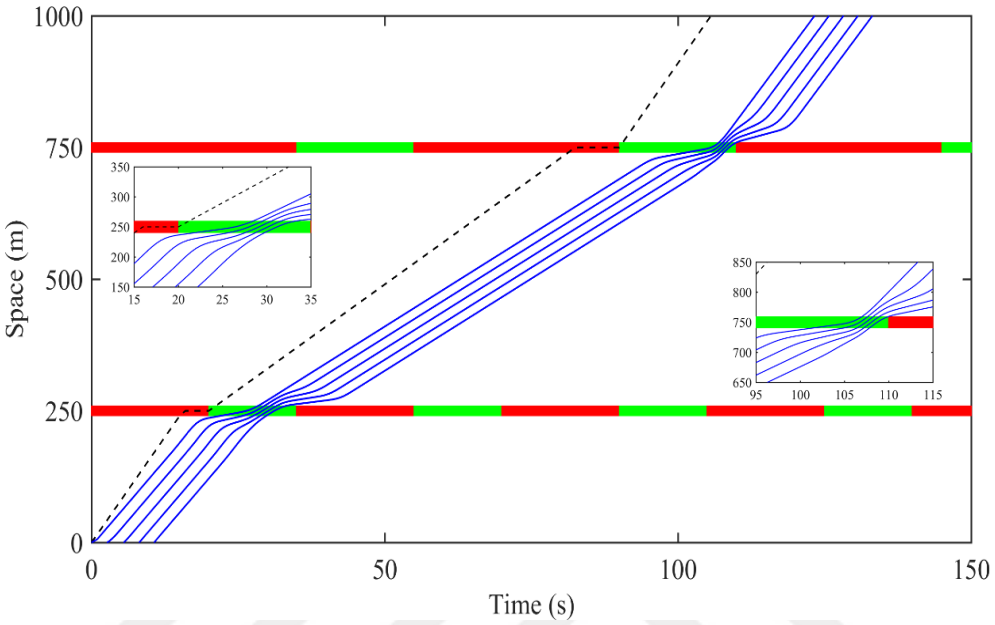


Figure 4.13: Optimal vehicle trajectories by using mode '1+m(w)' with enforcing speed limit for leading vehicle in transition process

Trajectories and speed of AVs can be changed to find optimal solution with minimum system level emission objectives or energy consumption based on the corresponding speed-related polynomial cost function (e.g. [80]). While human-driving vehicles have to wait at intersections (shown was dash lines), all AVs can pass through the intersections without waiting by reducing reaction time and optimized speed along the journey. Since the reaction time and speed have been changed at different segments to find the optimal solution, maximum service rates can be also calculated analytically at different locations. To derive more practically useful capacity estimation results under different communication standards, a more systematically designed study should be conducted to provide the guidelines using realistic settings and real-world geometry features. In addition, the last vehicle in Figure 4.12 appears to violate the speed limit. As noted in section 2.2, it is possible for the following vehicle when the reaction time is changeable in the state transition process. However, as a control variable, the speed of lead vehicle cannot exceed the maximum speed in this mode. Different simulation results can be obtained by assigning different settings such as enforcing speed limit for leading vehicle

in transition process in Figure 4.13. While the last vehicle in the platoon can speed up to catch up leading vehicle in Figure 4.12, the last vehicle keeps its speed and the leading vehicles slowdown in transition process in Figure 4.13.

It should be remarked that, the solution obtained by DP may be just one of optimal solutions to reach system-level minimal travel cost. The result with an optimal reaction time greater than the minimum reaction time can improve the safety, to some extent, when using an unchanged minimum reaction time can also reach the minimal system cost.

CHAPTER 5

RESULTS AND CONCLUSION

5.1 Answers to the research questions

The main focus of this research was to present a novel control strategy for autonomous and connected vehicles. The answers to the research questions of this research have been given as below:

1) How to adapt the current car-following models to model traffic interactions of automated vehicles based on available connectivity and automated functions, and in particular the dynamic process of tight platoon formation and system-level control?

This study constructs a family of efficient optimization models and algorithms to embed vehicle kinematics and minimum safe distance between consecutive following vehicles by using extended Newell's simplified car-following model. The main advantage of the proposed model is to enhance the service rate by adjusting vehicle trajectory speed and system level platoon reaction time at critical bottlenecks. Unlike similar control strategies, which handle only closed boundary conditions, the proposed model solves efficiently semi-open boundary conditions by using dynamic programming models with travel time, throughput and fuel consumption optimization objectives. The two aspects namely (i) adjustment of system level reaction time in discretized space-time-reaction time network and (ii) focusing on the optimality of system through controlling simultaneously all vehicles in the platoon, contribute new knowledge to the existing vehicle trajectory optimization studies.

2) How to develop a theoretically rigorous optimization model (e.g., in the form of dynamic programming models) which could be programmable using different programming languages? Desirable multi-vehicle trajectory optimization models should be able to not only satisfy critical operational constraints such as obstacle avoidance, but

also recognize the inherent nature of car following behavior to optimize platoon-level or system-level performance.

The results of numerical experiments have revealed efficiency of controlling reaction time as a new control variable, and increasing system level flexibility and optimality by forming vehicle platoons adaptively at critical bottlenecks. Also, these results give projections for communication connectivity considering team based safety when reaction time dynamically changes under communication support conditions. The approaches for dynamic programming under typical time-dependent bottleneck scenarios are examined to show the benefits of optimizing AVs trajectories with achievement of desired goals.

3) How to design on-line trajectory optimization algorithms to improve the performance of coupled AVs in a platoon, under complex traffic conditions with time-dependent capacity bottlenecks and obstacles of moving trajectories?

Through the numerical experiments for configuring platoon level reaction time under complex driving conditions by using real world trajectories data, it can be noted that multiple AVs increase the service rate under supported communication conditions.

5.2 Future works and discussions

Future work will mainly focus on (i) using backward and forward DP algorithms to better refine the feasible space prim and iteratively search the feasible ending states for ultimate optimal solutions, (ii) better selecting the discretization granularity for our multi-dimensional discretized networks, (iii) smoothing vehicle trajectories generated by Newell's car-following model, (iv) performance evaluation of the current model by using different car-following models, (v) developing the merge-diverge algorithms for different platoon level of multiple AVs, (vii) developing control models for the formation of swarms consisting of multiple AVs in a large scale application.

REFERENCES

[1] Herman, R., & Ausubel, J. H. (Eds.). (1988). Cities and their vital systems: Infrastructure past, present, and future. National Academies Press.

[2] Manyika J, Chui M, Bughin J, Dobbs R, Bisson P, Marrs A (2013) Disruptive technologies: advances that will transform life, business, and the global economy. McKinsey Global Institute New York.

[3] Zheng, K., Zheng, Q., Yang, H., Zhao, L., Hou, L., & Chatzimisios, P. (2015). "Reliable and efficient autonomous driving: the need for heterogeneous vehicular networks.", IEEE Communications Magazine, 53(12): 72-79.

[4] National Highway Traffic Safety Administration. (2016). Federal Automated Vehicles Policy: Accelerating the Next Revolution in Roadway Safety. United States Department of Transportation, Washington, DC.

[5] SAE International, U.S. Department of Transportation's New Policy on Automated Vehicles Adopts SAE International's Levels of Automation for Defining Driving Automation in On-Road Motor Vehicles, http://articles.sae.org/15021, 10 June 2017.

[6] Varaiya, P., (1993). "Smart cars on smart roads: problems of control." IEEE Transactions on automatic control, 38(2):195-207.

[7] Mahmassani, H. S., (2016). "50th Anniversary Invited Article—Autonomous Vehicles and Connected Vehicle Systems: Flow and Operations Considerations", Transportation Science, 50(4), 1140-1162.

[8] Reuschel, A., (1950). "Vehicle Movements in a Platoon." Oesterreichisches Ingenieur-Archir, 4:193-215.

[9] Pipes, L.A., (1953). "An Operational Analysis of Dynamics", Journal of Applied Physics, 24, No.3:274-287.

[10] Kometani, E., & Sasaki, T., (1958). "On the stability of traffic flow (report-I)", Journal of Operations Research Japan, 2(1):11-26.

[11] Kometani, E., & Sasaki, T., (1959). "A safety index for traffic with linear spacing", Operations research, 7(6):704-720.

[12] Kometani, E. & Sasaki, T., (1961), "Dynamic Behavior of Traffic with a Non-linear Spacing-Speed Relationship", Theory of Traffic Flow Symposium Proceeding, 1:105-119.

[13] Forbes, T. W., Zagorski, H. J., Holshouser, E. L., & Deterline, W. A., (1958). "Measurement of driver reactions to tunnel conditions", In Highway Research Board Proceedings, 37:345-357.

[14] Forbes, T. W., (1963). “Human factor considerations in traffic flow theory”, Highway Research Record, 15:60-66.

[15] Chandler, R. E., Herman, R., & Montroll, E. W., (1958). “Traffic dynamics: studies in car following”, Operations research, 6(2):165-184.

[16] Newell, G. F., (1993). “A simplified theory of kinematic waves in highway traffic, part I: General theory”, Transportation Research Part B: Methodological, 27(4):281-287.

[17] Newell, G. F., (2002). “A simplified car-following theory: a lower order model”, Transportation Research Part B: Methodological, 36(3):195-205.

[18] Ahn, S., Cassidy, M. J., & Laval, J., (2004). “Verification of a simplified car-following theory”, Transportation Research Part B: Methodological, 38(5):431-440.

[19] Taylor, J., Zhou, X., Rouphail, N. M., & Porter, R. J., (2015). “Method for investigating intradriver heterogeneity using vehicle trajectory data: a dynamic time warping approach”, Transportation Research Part B: Methodological, 73:59-80.

[20] Hamdar, S. H., Treiber, M., & Mahmassani, H. S. (2009). “Calibration of a stochastic car-following model using trajectory data: exploration and model properties.” In Transportation Research Board 88th Annual Meeting, 11-15 January 2009, Washington DC.

[21] Laval, J. A., & Leclercq, L., (2010). “A mechanism to describe the formation and propagation of stop-and-go waves in congested freeway traffic”, Philosophical Transactions of the Royal Society of London A: Mathematical, Physical and Engineering Sciences, 368(1928):4519-4541.

[22] Hoogendoorn, S., Hoogendoorn, R., & Daamen, W., (2011). “Wiedemann revisited: new trajectory filtering technique and its implications for car-following modeling”, Transportation Research Record: Journal of the Transportation Research Board, 2260:152-162.

[23] Kim, J., & Mahmassani, H., (2011). “Correlated parameters in driving behavior models: car-following example and implications for traffic microsimulation”, Transportation Research Record: Journal of the Transportation Research Board, 2249: 62-77.

[24] Ward, J. D., (1997). “Step by Step to an Automated Highway System-And Beyond.” In Automated Highway Systems, Springer US, 1:73-91.

[25] Horowitz, R., & Varaiya, P., (2000). “Control design of an automated highway system”, Proceedings of the IEEE, 88(7):913-925.

[26] National Automated Highway System Consortium (NAHSC), Milestone 2 Reporter, (1996) Hard Braking Safety Analysis Method and Detailed Results, Appendix J, 17.

[27] Bose, A., & Ioannou, P., (1999). “Analysis of traffic flow with mixed manual and semi-automated vehicles”, In American Control Conference, 1999. Proceedings of the 1999, IEEE, 3:2173-2177.

[28] Alvarez, L., & Horowitz, R., (1999). “Safe platooning in automated highway systems part I: Safety regions design”, Vehicle System Dynamics, 32(1): 23-55.

[29] Lioris, J., Pedarsani, R., Tascikaraoglu, F.Y. and Varaiya, P., (2017). "Platoons of connected vehicles can double throughput in urban roads", Transportation Research Part C: Emerging Technologies, 77:292-305.

[30] Treiber, M., Hennecke, A., & Helbing, D., (2000). "Congested traffic states in empirical observations and microscopic simulations", Physical review E, 62(2):1805-1824.

[31] Milanés, V., & Shladover, S. E., (2014). "Modeling cooperative and autonomous adaptive cruise control dynamic responses using experimental data", Transportation Research Part C: Emerging Technologies, 48:285-300.

[32] Talebpour, A., & Mahmassani, H. S., (2015). "Influence of Autonomous and Connected Vehicles on Stability of Traffic Flow", In Transportation Research Board 94th Annual Meeting, 11-15 January 2015, Washington DC.

[33] Roncoli, C., Papageorgiou, M., & Papamichail, I., (2015a). "Traffic flow optimization in presence of vehicle automation and communication systems–Part I: A first-order multi-lane model for motorway traffic", Transportation Research Part C: Emerging Technologies, 57:241-259.

[34] Roncoli, C., Papageorgiou, M., & Papamichail, I., (2015b). "Traffic flow optimization in presence of vehicle automation and communication systems–Part II: Optimal control for multi-lane motorways", Transportation Research Part C: Emerging Technologies, 57:260-275.

[35] Hu, J., Shao, Y., Sun, Z., Wang, M., Bared, J., & Huang, P., (2016). "Integrated optimal eco-driving on rolling terrain for hybrid electric vehicle with vehicle-infrastructure communication", Transportation Research Part C: Emerging Technologies, 68:228-244.

[36] Askari, A., Farias, D., Kurzhanskiy, K., Varaiya, P., (2017). "Effect of Adaptive and Cooperative Adaptive Cruise Control on Throughput of Signalized Arterials", In IEEE Intelligent Vehicles Symposium (IV), 11-14 June 2017, California.

[37] Betts, J. T. (1998). "Survey of numerical methods for trajectory optimization." Journal of guidance, control, and dynamics", Journal of guidance, control, and dynamics, 21(2):193-207.

[38] He, X., Liu, H. X., & Liu, X., (2015). "Optimal vehicle speed trajectory on a signalized arterial with consideration of queue", Transportation Research Part C: Emerging Technologies, 61:106-120.

[39] Wu, X., He, X., Yu, G., Harmandayan, A., & Wang, Y., (2015). "Energy-optimal speed control for electric vehicles on signalized arterials", IEEE Transactions on Intelligent Transportation Systems, 16(5):2786-2796.

[40] Schouwenaars, T., De Moor, B., Feron, E., & How, J., (2001). "Mixed integer programming for multi-vehicle path planning". In IEEE Control Conference (ECC), 4-7 September 2001, Porto, (2603-2608).

[41] Grøtli, E. I., & Johansen, T. A., (2012). "Path planning for UAVs under communication constraints using SPLAT! and MILP", Journal of Intelligent & Robotic Systems, 65(1-4):265-282.

[42] Grøtli, E. I., & Johansen, T. A., (2016). "Motion-and Communication-Planning of Unmanned Aerial Vehicles in Delay Tolerant Network using Mixed-Integer Linear Programming", Modeling, Identification and Control, 37(2):77-97.

[43] Richards, A., Bellingham, J., Tillerson, M., & How, J., (2002). "Coordination and control of multiple UAVs.", In AIAA guidance, navigation, and control conference, 6-8 August 2002, Monterey, CA.

[44] Sun, X., & Cassandras, C. G., (2016). "Optimal dynamic formation control of multi-agent systems in constrained environments", Automatica, 73:169-179.

[45] Flint, M., Polycarpou, M., & Fernandez-Gaucherand, E., (2002). "Cooperative path-planning for autonomous vehicles using dynamic programming", In Proceedings of the IFAC 15th Triennial World Congress, 21-26 July 2002, Barcelona, (1694-1699).

[46] McNaughton, M., (2011). Parallel algorithms for real-time motion planning, Ph.D. dissertation, Carnegie Mellon University, Pittsburgh, Pennsylvania.

[47] Urmson, C., Anhalt, J., Bagnell, D., Baker, C., Bittner, R., Clark, M. N., ... & Gittleman, M., (2008). "Autonomous driving in urban environments: Boss and the urban challenge", Journal of Field Robotics, 25(8):425-466.

[48] Katrakazas, C., Quddus, M., Chen, W. H., & Deka, L., (2015). "Real-time motion planning methods for autonomous on-road driving: State-of-the-art and future research directions", Transportation Research Part C: Emerging Technologies, 60:416-442.

[49] Paden, B., Cap, M., Yong, S. Z., Yershov, D., & Frazzoli, E., (2016). "A Survey of Motion Planning and Control Techniques for Self-driving Urban Vehicles", IEEE Transactions on Intelligent Vehicles, 1(1):33-55.

[50] Zhou, F., Li, X., & Ma, J., (2017). "Parsimonious shooting heuristic for trajectory design of connected automated traffic part I: Theoretical analysis with generalized time geography", Transportation Research Part B: Methodological. 95:394-420.

[51] Ma, J., Li, X., Zhou, F., Hu, J., & Park, B. B., (2016). "Parsimonious shooting heuristic for trajectory design of connected automated traffic part II: Computational issues and optimization", Transportation Research Part B: Methodological, 95:421-441.

[52] Bang, S., Ahn, S. (2017). "Platooning Strategy for Connected and Autonomous Vehicles: Transition From Light Traffic." the 96th 10 Transportation Research Board Annual Meeting, Paper ID: 17-02010.

[53] Yanakiev, D. and Kanellakopoulos, I., (1998). "A simplified framework for string stability analysis of automated vehicles", Vehicle System Dynamics, 30: 375-405.

[54] Munigety, C. R., Gupta, P. A., Gurumurthy, K. M., Peeta, S., and Mathew, T. V., (2016). "Vehicle- type Dependent Car following Model Using Spring-mass-damper Dynamics for Heterogeneous Traffic", The 95th Transportation Research Board Annual Meeting, 11-15 January 2016, Washington DC.

[55] Gong, S., Shen, J. and Du, L., (2016). "Constrained optimization and distributed computation based car following control of a connected and autonomous vehicle platoon", Transportation Research Part B: Methodological, 94:314-334.

[56] LaValle, S. M., (2006). Planning algorithms, First Edition, Cambridge University Press, Cambridge.

[57] Murray, R. M., (2007). "Recent research in cooperative control of multivehicle systems", Journal of Dynamic Systems, Measurement, and Control, 129(5):571-583.

[58] Chen, Y. Q., & Wang, Z., (2005). "Formation control: a review and a new consideration", In IEEE Intelligent Robots and Systems, 2-6 August 2005, Alberta, Canada, (3181-3186).

[59] Balch, T., & Arkin, R. C., (1998). "Behavior-based formation control for multirobot teams", IEEE transactions on robotics and automation, 14(6):926-939.

[60] Egerstedt, M., & Hu, X., (2001). "Formation constrained multi-agent control", IEEE transactions on robotics and automation, 17(6):947-951.

[61] Stentz, A., (1994). "Optimal and efficient path planning for partially-known environments", In IEEE International Conference on Robotics and Automation, 8-13 May 1994, San Diego, (3310-3317).

[62] Guo, Y., & Parker, L. E., (2002). "A distributed and optimal motion planning approach for multiple mobile robots", In IEEE International Conference on Robotics and Automation, 11-15 May 2002, Washington DC, (3:2612-2619).

[63] Kanayama, Y., Kimura, Y., Miyazaki, F., Noguchi, T., (1990). "A stable tracking control method for an autonomous mobile robot", In IEEE International Conference on Robotics and Automation, 13-18 May 1990, Cincinnati, Ohio, (384-389).

[64] De Wit, C.C., Sordalen, O.J., (1992). "Exponential stabilization of mobile robots with nonholonomic constraints", IEEE transactions on automatic control, 37(11):1791-1797.

[65] Miao, Z., Wang, Y., (2015). "Adaptive Control for Simultaneous Stabilization and Tracking of Unicycle Mobile Robots", Asian Journal of Control, 17(6):2277-2288.

[66] Przybyla, J., Taylor, J., Jupe, J., & Zhou, X., (2015). "Estimating risk effects of driving distraction: a dynamic errorable car-following model", Transportation Research Part C: Emerging Technologies, 50:117-129.

[67] Wei, Y., Liu, J., Li, P., & Zhou, X., (2016). "Longitude trajectory optimization for autonomous vehicles: An approach based on simplified car-following model", In Transportation Research Board 95th Annual Meeting, 11-15 January 2016, Washington DC.

[68] Ioannou, P. A. et al, (1994). Activity D: Lateral and longitudinal control analysis. Final Report.

[69] Bose, A., & Ioannou, P. A., (2003). "Analysis of traffic flow with mixed manual and semiautomated vehicles", IEEE Transactions on Intelligent Transportation Systems, 4(4):173-188.

[70] Kesting, A., Treiber, M., Helbing, D., (2010). "Connectivity statistics of store-and-forward inter-vehicle communication", IEEE Trans. Intell. Transp. Syst. 11:172–181.

[71] Jia, D., & Ngoduy, D., (2016a). “Platoon based cooperative driving model with consideration of realistic inter-vehicle communication”, Transportation Research Part C: Emerging Technologies, 68:245-264.

[72] Jia, D., & Ngoduy, D., (2016b). “Enhanced cooperative car-following traffic model with the combination of V2V and V2I communication”, Transportation Research Part B: Methodological, 90:172-191.

[73] Bai, F., & Krishnan, H., (2006). “Reliability analysis of DSRC wireless communication for vehicle safety applications.” In IEEE Intelligent Transportation Systems Conference, 17-20 September 2006, Toronto, Ontario, (pp. 355-362).

[74] Xu, L., Wang, L. Y., Yin, G., & Zhang, H., (2014). “Communication information structures and contents for enhanced safety of highway vehicle platoons”, IEEE Transactions on Vehicular Technology, 63(9):4206-4220.

[75] Cheng, X., Chen, C., Zhang, W., & Yang, Y., (2017). “5G-Enabled Cooperative Intelligent Vehicular (5GenCIV) Framework: When Benz Meets Marconi”, IEEE Intelligent Systems, 32(3): 53-59.

[76] Bellman, R. E., (1957). Dynamic Programming, Princeton University Press, Princeton, New Jersey.

[77] Jensen, P. A., & Bard, J.F., (2003). Operations research models and methods, Volume 1, John Wiley & Sons Incorporated, Massachusetts.

[78] Bradley, S., Hax, A., & Magnanti, T. (1977). Applied mathematical programming, First Edition, Addison-Wesley, Boston, Massachusetts.

[79] Zhou L, Tong L, Chen J, Tang J, Zhou X., (2017). “Joint optimization of high-speed train timetables and speed profiles: A unified modeling approach using space-time-speed grid networks”, Transportation research part B: Methodological 97:157-181.

[80] Ma, R., Ban, X. J., & Szeto, W. Y., (2015). “Emission modeling and pricing in dynamic traffic networks”, Transportation Research Procedia, 9:106-129.

[81] US Department of Transportation (USDOT), 2006-NGSIM – Next Generation Simulation, http://ops.fhwa.dot.gov/trafficanalysistools/ngsim.html, 01 March 2018.

[82] Aziz, H. M. A. and Ukkusuri, S. V., (2012), “Integration of Environmental Objectives in a System Optimal Dynamic Traffic Assignment Model”, Computer-Aided Civil and Infrastructure Engineering, 27:494–511.

[83] Leclercq, L., Laval, J. A.,& Chiabaut, N., (2011). “Capacity drops at merges: An endogenous model”, Transportation Research Part B: Methodological, 45:1302–1313.

[84] Chen, X. M., Li, Z., Li, L., & Shi, Q., (2014). ”A traffic breakdown model based on queueing theory”, Networks and Spatial Economics, 14(3-4):485-504.

[85] Fukutome, I., & Moskowitz, K., (1960). “Traffic behavior and on-ramp design”, Highway Research Board Bulletin, 235:38–72.

[86] Harwood, D.W., & Mason, J. M., (1993). “Ramp/mainline speed relationships and design considerations”, Transportation Research Record, 1385:121–125.

[87] Hunter, M., Machemehl, R., & Tsyganov, A., (2001). “Operational evaluation of freeway ramp design”, Transportation Research Record: Journal of the Transportation Research Board, 1751:90–100.

[88] Papageorgiou, M., & Kotsialos, A., (2002). “Freeway ramp metering: An overview”, IEEE Transactions on Intelligent Transportation Systems, 3:271–281.

[89] Ntousakis, I. A., Nikolos, I. K., & Papageorgiou, M., (2016). “Optimal vehicle trajectory planning in the context of cooperative merging on highways”, Transportation Research Part C: Emerging Technologies, 71:464-488.

APPENDIX-A

POSSIBLE EXTENSION TO MULTI-PLATOON MERGING CONTROL

Congestion on motorways is a phenomenon affecting society, the economy and the environment. It often takes place at specific locations such as onramps, lane drops, crests, sags and sharp bends. Particularly recurrent and degrading for the infrastructure is congestion at on-ramps, which can cause a drop in capacity and blockages of upstream off-ramps [81, 82, 83]. Research on the management and avoidance of this phenomenon has been carried out since the development of motorway roads. Initial attempts to decrease and prevent congestion at merges were related to the physical improvement of the infrastructure layout, trying to identify the optimal junction design [84, 85, 86]. Subsequently, the attention moved to active traffic management (ATM) strategies, and systems such as ramp metering have been introduced to control on-ramp flows and avoid or at least delay breakdown on the main carriageway [87, 88]. These new control strategies are based on emerging V2V and V2I communication technologies, more accurate positioning systems, in-car driver assistance devices and on a better understanding of traffic flow phenomena. These advances open new possibilities in the field of ATM, and particularly promising is the cooperation among vehicles enabled by the V2V and V2I communication.

The merging process in human operated vehicle environment consists of the following three steps: choosing possible gap for the adjacent target lane, adjusting speed, and performing required maneuvers [89]. As a simple conceptual illustration, the merging process in AV environment can be performed with satisfying desired objectives and ensuring safety constraints. We can provide optimized solution for merging process by controlling all AVs in on-ramp and mainstream, and by defining different reaction times for platoon level (τ_p) and system level (τ_s).

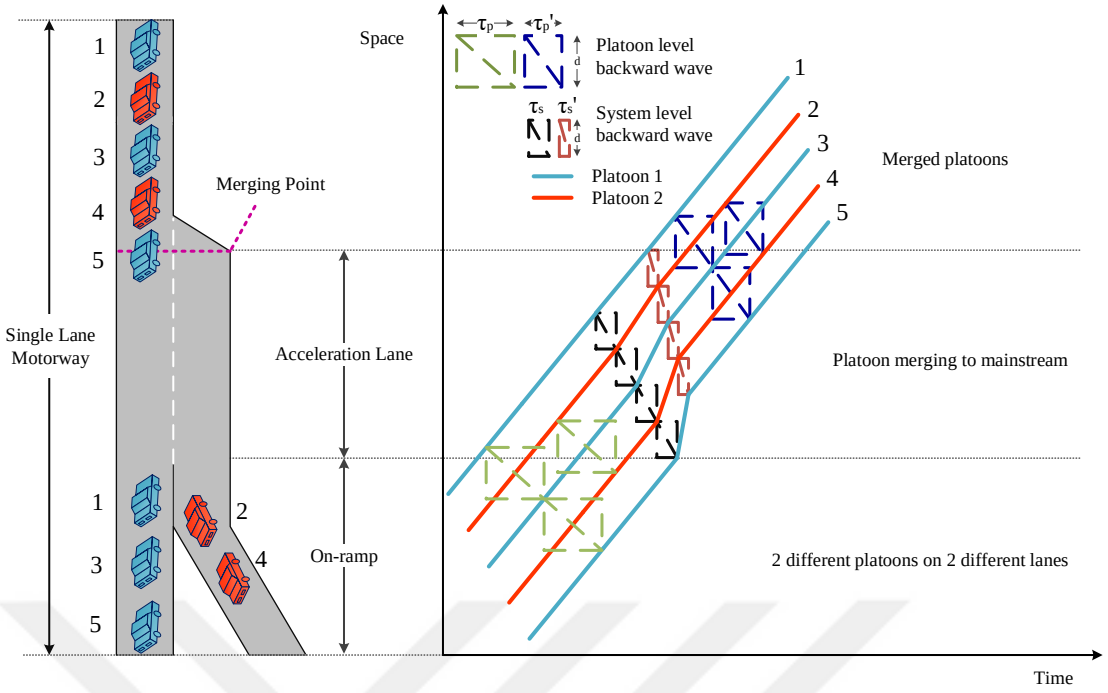


Figure A.1. Illustration of merging process by using multi-platoon formation control

As shown in Figure A.1, there are two different platoons before merging consisting of 3 and 2 AVs, respectively. In this merging process, the system level reaction time is symmetrically adjusted to meet distance headway constraints between vehicles from two different platoons. In our illustrative example, the merging point is assumed to be the end of the acceleration lane.

CURRICULUM VITAE

PERSONAL INFORMATION

Name Surname : Cafer AVCI

Date of birth and place : 1985, Bursa, Turkey

Foreign Languages : English

E-mail : cafer.avci@yalova.edu.tr

EDUCATION

Degree	**Department**	**University**	**Date of Graduation**
Master	Computer Engineering	Yalova University	2012
Undergraduate	Computer and Control Technology (English)	Marmara University	2009
High School	Computer Science	Tophane Anatolian Technical High School	2004

WORK EXPERIENCE

Year	**Corporation/Institute**	**Enrollment**
2017	Civil and Environmental Engineering, Arizona State University	Visiting Scholar

2013	Mihman Technology, High Tech Zone, Uludag University,	Founder
2011	Computer Engineering, Yalova University	Research Asisstant
2010	Computer Engineering, Kocaeli University	Research Asisstant

PUBLISHMENTS

Papers

[1] Wei Y., Avcı C., Liu J., Belezamo B., Aydın N., Li P.(Taylor), Zhou X., (2017). "Dynamic programming-based multi-vehicle longitudinal trajectory optimization with simplified car following models", Transportation Research Part B: Methodological, 106:102-129.

[2] Avcı C., Akbas A. (2015). "Sleep Apnea Classification Based on Respiration Signals by Using Ensemble Methods", Bio-Medical Materials and Engineering, 26(1):1703-1710.

Conference Papers

[1] Ilhan H.O. and Avcı C., (2017). "Sleep stage classification by ensemble learning methods with active sample selection techniques", International Artificial Intelligence and Data Processing Symposium (IDAP), 16-17 September 2017, Malatya, Turkey.

[2] Avcı, C. and Akbas A., (2015). "Review of Multiagent Systems in Traffic Management Systems", 3rd. International Istanbul Smart Grid Congress and Fair (ICSG 2015), 29-30 April 2015, Istanbul, Turkey.

[3] Avcı C., Akbas A. and Yuksel Y., (2014). "Evaluation of statistical metrics by using physiological data to identify the stress level of drivers", The International Conference on Future Bioengineering (ICFB 2014), 13-14 December 2014, Kuala Lumpur, Malaysia.

[4] Akbaş, A., Avcı, C., Delibaşoğlu, İ., Karakullukçu, B., (2014). "On The Design of the Architecture of National ITS System", 1st National Congress and Exhibition on Intelligent Transport Systems for Highways (KAUS 2014), 26-28 May 2014, Istanbul, Turkey.

[5] Avcı C., Bilgin G., (2013). "Sleep Apnea Detection using Adaptive Neuro Inference System", The 7th International Conference on Bioinformatics and Biomedical Engineering (ICBBE 2013), 26-28 September 2013, Beijing-China.

[6] Akbaş A., Turhal U., Babur S. and Avcı C., (2013). "Performance Improvement with Combining Multiple Approaches to Diagnosis of Thyroid Cancer", The 7th International Conference on Bioinformatics and Biomedical Engineering (ICBBE 2013), 26-28 September 2013, Beijing-China.

[7] Turhal U., Babur S., Avcı C., Akbas A., (2013). "Performance Improvement for Diagnosis of Colon Cancer by Using Ensemble Classification Methods", The International Conference on Technological Advances in Electrical, Electronics and Computer Engineering (TAEECE 2013), 9-11 May 2013, Konya-Turkey.

[8] Tekin M., Avcı C., Akbas A., (2012). "Parkinson Disease Classification Based On Wavelet Analysis" The 9th International Conference on Electronics, Computer and Computation (ICECCO 2012), 1-3 November 2012, Ankara-Turkey.

[9] Kosesoy I., Gok M., Avcı C., (2012). "Comparison Among Feature Encoding Techniques for HIV-1 Protease Cleavage Site Prediction", The 9th International

Conference on Electronics, Computer and Computation (ICECCO 2012), 1-3 November 2012, Ankara-Turkey.

[10] Avcı C., Akbas A., (2012). "Real Time Sleep Apnea Detection with Wavelet Decomposition of Respiratory Signals", The 6th International Conference on Bioinformatics and Biomedical Engineering (iCBBE 2012), 17-20 May 2012, Shanghai-China.

[11] Avcı C., Delibasoglu I., Akbas A., (2012). "Sleep Apnea Detection Using Wavelet Analysis of ECG Derived Respiratory Signal", The International Conference on Biomedical Engineering (ICOBE 2012), 27-28 February 2012, Perlis-Malaysia.

[12] Avcı C., Akbas A., (2012). "Comparison of the ANN Based Classification accuracy for real time sleep apnea detection methods", The 9th International Conference on Biomedical Engineering (BIOMED 2012), 15-17 February 2012, Innsbruck-Austria.

[13] Delibasoglu, I., Avcı, C., Akbas, A., (2011). "ECG Based Sleep Apnea Detection Using Wavelet Analysis of Instantaneous Heart Rates", 4th International Symposium on Applied Sciences in Biomedical and Communication Technologies (ISABEL 2011), 26-29 October 2011, Barcelona, Spain.

[14] Avcı, C., Besli, S., Akbas, A., (2011). "Performance of the EDR Methods; Evaluations using the mean and instantaneous respiratory rates", The 5th International Conference on Bioinformatics and Biomedical Engineering (ICBBE 2011), 10-12 May 2011, Wuhan-China.

Projects

[1] Designing and Planning of the Architecture of Intelligent Transportation System, Republic of Turkey, Ministry of Transport Maritime Affairs and Communications, General Directorate of Highways, Researcher, 2014.

[2] An Embedded System Design for the Preprocessing of Analog Signals in the Patient Monitoring System, 2014/BAP/080, Yalova University, Researcher, 2014.

[3] Designing of the ECG Holter Equipment, Republic of Turkey, Ministry of Science, Industry and Technology, Entrepreneur & Researcher, 2013.

[4] IP Based Patient Monitoring System, 2012/YL/002, Yalova University, Researcher, 2012.